frontiers | Frontiers in Marine Science

TYPE Original Research
PUBLISHED 24 February 2025
DOI 10.3389/fmars.2025.1519179

Check for updates

OPEN ACCESS

EDITED BY
Ce Wang,
Sun Yat-sen University, China

REVIEWED BY
Qiangtai Huang,
Sun Yat-sen University, China
Lynn Dafoe,
Geological Survey of Canada, Canada

*CORRESPONDENCE
Detian Yan
yandetian@cug.edu.cn

RECEIVED 29 October 2024
ACCEPTED 29 January 2025
PUBLISHED 24 February 2025

CITATION
Li T, Yan D, Liu E, Zhang J, Wei X, Lu Z and Lin X (2025) Patterns of shelf margin clinoform: control of the development of deep-water sedimentary systems.
Front. Mar. Sci. 12:1519179.
doi: 10.3389/fmars.2025.1519179

COPYRIGHT
© 2025 Li, Yan, Liu, Zhang, Wei, Lu and Lin. This is an open-access article distributed under the terms of the Creative Commons Attribution License (CC BY). The use, distribution or reproduction in other forums is permitted, provided the original author(s) and the copyright owner(s) are credited and that the original publication in this journal is cited, in accordance with accepted academic practice. No use, distribution or reproduction is permitted which does not comply with these terms.

Patterns of shelf margin clinoform: control of the development of deep-water sedimentary systems

Tong Li[1,2,3], Detian Yan[1,2,3]*, Entao Liu[4], Junfeng Zhang[1,2,3], Xiaosong Wei[1,2,3], Zeyu Lu[1,2,3] and Xudong Lin[4]

[1]School of Earth Resources, China University of Geosciences, Wuhan, China, [2]Key Laboratory of structure and Oil and Gas Resources, Ministry of Education, China University of Geosciences (Wuhan), Wuhan, China, [3]Hubei Key Laboratory of Oil and Gas Exploration and Development Theory and Technology (China University of Geosciences), Wuhan, China, [4]Hubei Key Laboratory of Marine Geological Resource, China University of Geosciences (Wuhan), Wuhan, China

The clinothem is the fundamental element of basin infill and plays an important role in the source-to-sink system of deep-water basins. In this study, which is based on 2D and 3D seismic data, the spatiotemporal evolution of clinothems and depositional systems from the Miocene to the Pleistocene in the Qiongdongnan Basin, northern South China Sea, is investigated. The following conclusions are drawn: (1) three variations of clinothems in the Qiongdongnan Basin were recognized respective O-, S- and F-type clinothems; (2) fluctuations in the relative base level, in combination with variations in sediment supply, result in different clinothem patterns that may be used to understand changes in these depositional factors; and (3) the development of O-type clinothem is usually accompanied by slope instability and slumping, leading to mass transport deposits on the basin plain. When suitable transport pathways exist (e.g., shelf canyons) on the shelf-edge or when the F-type clinothem develops, sediments can be dispersed basinward, promoting submarine fan development. Results from this study will help in understanding the sedimentological development of slope and basin plain areas and offers significant insights into the understanding of deep-sea depositional systems.

KEYWORDS

Qiongdongnan Basin, shelf-edge trajectory, clinothem, deep-water sedimentary system, quaternary

1 Introduction

Shelf-edge clinoforms facilitate sediment transport from shallow- to deep-water areas, play a crucial role in source-to-sink systems and have drawn attention in various global basin environments (Pellegrini et al., 2020). The development of clinothems is influenced by multiple factors, including interactions between relative sea level changes, accommodation space, and sediment supply. Clinothems are important for revealing

mechanisms of sediment transport into basins, aiding in palaeoenvironmental analysis and hydrocarbon reservoir exploration (Gong et al., 2016a; Patruno and Helland-Hansen, 2018; Gamberi et al., 2020; Patruno et al., 2020). Clinothems can also provide insights into global sea level fluctuations, indicating climate responses to sea level changes and sediment supply (Helland-Hansen and Hampson, 2009; Browning et al., 2013; Lin et al., 2018; Trincardi et al., 2020; Pellegrini et al., 2021, Pellegrini et al., 2024). Additionally, palaeogeographic and morphological studies of clinothems are important for understanding tectonic settings, with aggregational and progradational clinothems often associated with subsidence and uplift events (Bryn et al., 2020; Petersen, 2021).

In the marine system, a prograding shelf-edge, which advances seaward over a significant distance, allows transport of substantial amounts of coarse-grained terrigenous debris to the basin, forming submarine fan deposits, whereas a shelf-edge clinothem dominated by accumulation of sediment on the shelf exhibits the opposite characteristics, such as a lack of basin-associated deposits and submarine fans in the basin (Gomis-Cartesio et al., 2018; Cosgrove et al., 2020). In such cases, the application of sequence stratigraphy and shelf-edge trajectory analysis can provide a broader sight (Dafoe et al., 2023). Shelf-edge trajectory analysis can complement traditional sequence stratigraphy methods (Carvajal and Steel, 2006; Sanchez et al., 2012; Anell et al., 2014; Jones et al., 2015; Xu et al., 2018). This analysis aids in explaining the variations in sedimentary systems in deep basins during periods of high and low accommodation on the shelf, playing a crucial role in elucidating the changes in sedimentary systems specific to different geomorphic settings within the basin. Shelf-edge trajectory analysis allows for a better study of the dynamic evolution of sequences, focusing not only on the identification of key surfaces but also on the internal structural characteristics of the clinothem (Catuneanu et al., 2009).

The Qiongdongnan Basin (QDNB) is characterized by complex tectonic activity with a fast post-rift subsidence, an uneven sediment supply and diverse marine processes, making it a hotspot for offshore oil and gas exploration in China (Xie et al., 2008; Zhuo et al., 2019). The continental slope of the QDNB has developed since the late Miocene, with numerous studies focusing on (1) the accumulation and growth patterns of the shelf–slope system from the late Miocene to the Pleistocene (Gong et al., 2015; Zhao et al., 2019; Chen et al., 2020); (2) the impact of climate, hydrodynamics, sediment supply, and tectonic activities on the development of the shelf–slope system (Lin et al., 2018); and (3) the seismic reflection characteristics and quantitative analysis of clinothem parameters within the continental slope (Liu et al., 2023). Currently, there is still a lack of research on the evolutionary patterns of sedimentary systems under varying shelf-edge depositional trends.

The primary objectives of our current study are as follows: (1) illustrate the changes in shelf-edge trajectories and accumulation patterns during the late Miocene to Pleistocene evolution of the QDNB; (2) highlight the significance of sedimentological evolution of slope regions and deep-sea plains; and (3) show that clinothem patterns control the development and distribution of deep-water sedimentary system. The findings and techniques applied in this research are expected to aid in future quantitative assessments of the features and evolution of continental shelf margins globally.

2 Geological setting

The QDNB is located in the southeastern waters of Hainan Island (Wei et al., 2020) and is a rift-type oil- and gas-bearing basin formed by extensional tectonics along the passive continental margin of the northern South China Sea (Figure 1A). The basin formed during the middle to late Eocene rifting phase and a subsequent middle Miocene to present post-rifting phase (Morley, 2016; Zhao et al., 2018; Liang et al., 2020).

The shallow-water area of the QDNB has depths ranging from 0 to 200 m, transitioning to deeper-water regions beyond the shelf edge, where depths mostly exceed 2000 m. The QDNB is similar to most passive continental margin basins worldwide (Xie et al., 2006). These basins are influenced by extensional tectonic forces and are often associated with deep-sea sedimentation (Bauch et al., 2016; Septama et al., 2016; Zhang et al., 2019; Zhao et al., 2021). The continental shelf in the northern part of the South China Sea formed during the middle to late Miocene (Yuan et al., 2009; Jiang et al., 2015; Liu et al., 2022). The predominant sedimentary environment consists of a transition from the shallow sea to the deep sea (Cheng et al., 2023; Meng et al., 2021). In the study of the QDNB shelf margin, variations in the depositional trends along the shelf edge are believed to be linked to sea level changes, regional changes in tectonic setting, and sediment flux (Zhao et al., 2019; Zhuo et al., 2019; Chen et al., 2020). The growth of the continental margin in the QDNB during the Pliocene and the increased sediment flux are thought to have responded to the gradual cooling induced by icehouse periods and global sea-level lowering (Clift and Sun, 2006; Liu et al., 2010; Zhao et al., 2015). The western part of the basin is characterized by the infill of turbidite sand-rich canyons, whereas the eastern part is characterized by mass transport deposits originating from the northern slope (Li et al., 2021).

During the late Miocene to Pleistocene, the basin experienced a phase of rapid post-rift thermal subsidence (Figure 2). The Huangliu formation was deposited during the late Miocene. Seismic stratigraphic surface T40 is the boundary between the Huangliu Formation and Yinggehai Formation. The Yinggehai Formation developed during Pliocene, and surface T30 is the boundary between the Yinggehai and Ledong Formation. The boundary of Lower Ledong Formation and Lower Ledong Formation can be traced regionally on seismic profiles, referred to as the T14 surface. The main seismic stratigraphic surfaces and formations in QDNB were provided by the Research Institute of China National Offshore Oil Corporation, and the biochronologic stratigraphy of the QDNB was established based on calcareous microfossils in drilling cores has been established (Gong and Li, 1997). The seismic surfaces used in this study are T40, T30, T20 and T14. The unconformity surface T40 (10.5 Ma) is considered a crucial period marking the transition of the basin to a passive margin stage (Sun et al., 2010; Li et al., 2017; Lyu et al., 2021). The seismic stratigraphic surfaces overlying Huangliu Formation is T30 (5.5 Ma) (Sun et al., 2010; Liu et al., 2015). In the overlying

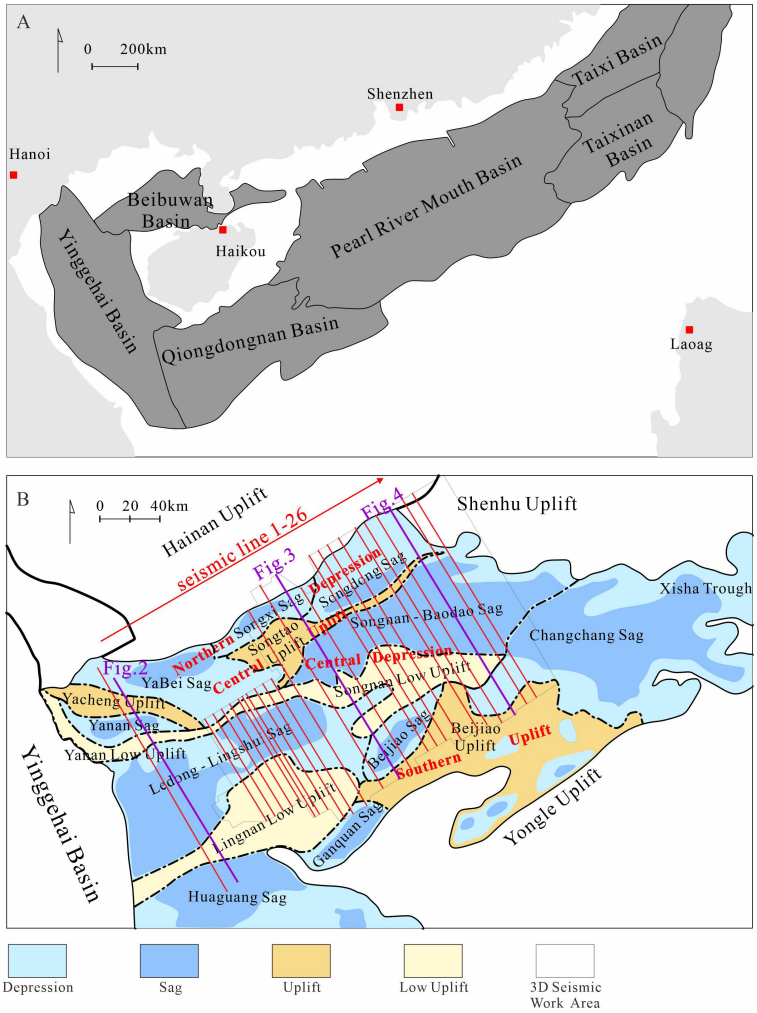

FIGURE 1
(A) Position of the Qiongdongnan Basin in its geographical and tectonic context. **(B)** Magnified view of seismic lines.

succession, the main seismic stratigraphic surfaces are T20 (1.8 Ma) and T14 (0.8 Ma) (Li et al., 2024). The dating mentioned above is crucial for this study.

3 Data and methods

In this study, 2D seismic reflection data and 3D seismic reflection data covering an area of approximately 20,000 km^2 are utilized (Figure 1B). The both 2D and 3D seismic data, acquired in 2009 and provided by the China National Offshore Oil Corporation Hainan Branch in 2022, were obtained via a 3000-metre-long streamer with 240 channels at a spacing of 12.5 metres. The vertical sampling rate is 2-4 ms, and both the inline and crossline spacings are 12.5 metres. The frequency of the focus of the seismic reflections in the targeted strata is 30–40 Hz.

The interpretation of seismic data was carried out by the Geoframe® software (a prudt of Schlumberger®). Building upon previous exploration and research findings, key seismic stratigraphic surface and stratigraphic positions were identified and delineated on the basis of unconformities, stratigraphic stacking relationships, and significant amplitude reflections along the chronostratigraphic axis. Mapping and nomenclature adhere to conventions established in prior exploration and research. The major seismic surfaces include T40 (11.6 Ma), T30 (5.5 Ma), T20 (1.8 Ma) and T14 (0.8 Ma), corresponding to the bottom of Huangliu, Yinggehai, Lower Ledong and Upper Ledong Formation respectively. The age of seismic surfaces were mainly derived from the biochronostratigraphy of CNOOC and previous studies (Gong and Li, 1997; Sun et al., 2010; Liu et al., 2015; Li et al., 2017; Li et al., 2024). Moreover, the RMS attribute map and Variance volume slices were extracted by the Geoframe® to reveal the plan-view characters of the sedimentary facies.

An essential element of this research is the division of the extensive succession of the continental margin in the QDNB into stratigraphic units that can be correlated and dated along the margin. To determine the clinoforms and shelf edge trajectories

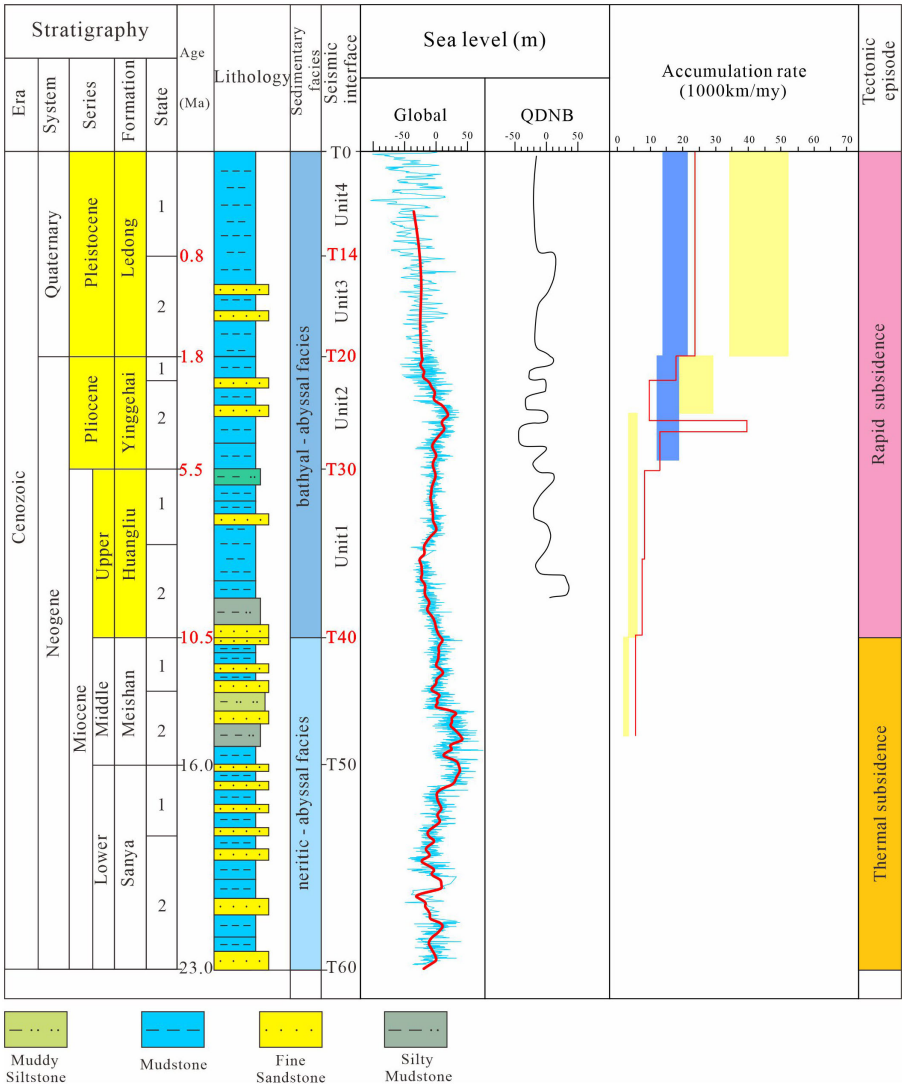

FIGURE 2
Stratigraphy of the study area. The formations in this study are coloured yellow. The sea-level fluctuations are modified after Miller et al. (2020). The relative sea level in the Qiongdongnan Basin is drawn after Zhao et al. (2019). The accumulation rate of QDNB (blue block is cited form Clift and Sun, 2006; yellow block is cited from van Hoang et al., 2010; red line is cited from Zhao et al., 2015). The tectonic spisode is modified after Cheng et al. (2021).

evolution characteristics, the quantitative parameters of the shelf edge trajectories in the study area were calculated and characterized via the method of calculating the trajectory angle proposed by Helland-Hansen and Hampson (2009). And the time-depth relation transforms formula has been used in time-to-depth conversion was provide by China National Offshore Oil Corporation:

$$\text{Depth} = 0.0002 * \text{TWT}^2 + 0.0752 * \text{TWT} \quad (1)$$

TWT is the Two-way travel time, ms.

The progradation and aggradation rates were calculated by:

$$\text{Rp} = \text{P}/\text{T} \quad (2)$$

Rp is the progradation rate, m/Myr; P is the prodradation distance, m; and T is the deposition time span of the slope, Myr.

$$\text{Ra} = \text{A}/\text{T} \quad (3)$$

Ra is the aggradation rate, m/Myr, A is the aggradation distance, m; and T is the deposition time span of the slope, Myr.

In addition, the classification method of clinothems is collected from the previous research results of Chen et al. (2018). The clinothem shapes have been defined by the changes in dominant thickness along any clinothem and this can change along-strike. They can be classified as F-type (Basin Floor Type) clinothem with thick basin floor deposits but relatively thin deposits on the shelf and deepwater slope; S-type (Slope Type) clinothem with relatively thick slope deposits but thinner deposits on both shelf and basin floor segments; and O-type (On the Shelf Type) clinothem with thick shelf deposits but relatively thin deposits on the slope and basin floor.

10.3389/fmars.2025.1519179

4 Results

4.1 Clinoforms, stacking patterns and shelf trajectories

Since the sedimentary period of Huangliu Formation, the slope in the QDNB has been continuously prograding towards the basin, resulting in the formation of a sedimentary body with a thickness exceeding 4 km above the bottom surface of Huangliu Fromation (Figure 3). Clinoforms advance progressively towards the basin, and the sedimentary layers accumulating on topset can characterize repeated transgressions and regressions of the coastline during growth of the shelf, leading to retrogradation.

The AA' seismic line, situated outside the three-dimensional seismic working area, represents a high-quality 2D seismic line that comprehensively captures the stratigraphic stacking patterns of the western shelf–slope–deep-sea plain in the southeastern QDNB (Figure 3). Between the T40 and T30 surface the clinothem is in a distinct progradational stage (Figure 3). Between the T30 and T20 surface (Figure 3), as a result of repeated shelf edge progradation, the trajectory prominently rises. The clinothem display a stacking pattern characterized by initial aggradation followed by progradation. Between the T20 surface up to the seafloor, the clinothem underwent a distinctive pattern of progradation followed by aggradation. Accordingly, there is a pronounced etendency for aggradation on the slope. This seismic profile in western QDNB show that clinoform is categorized into three distinct stages: a progradational phase characterized by descending shelf-edge trajectories (e.g., Huangliu Formation), exhibiting an average angle of 0.38°; a progradational and aggradational phase characterized by low-angle ascending shelf-edge trajectories (e.g., Yinggehai and Lower Ledong Formation), exhibiting an average angle of 2.90°; and an aggradational phases characterized by high-angle ascending trajectories (e.g., Upper Ledong Formation), exhibiting an average angle of 3.36°.

On the BB' seismic line, the shelf-edge trajectories exhibit an ascending pattern (Figure 4). Notably, the trajectory pattern on this profile is similar to that of the AA' seismic line. In the central part of the QDNB, the clinoform is subdivided into three stages: a progradational phase characterized by descending shelf-edge trajectories, exhibiting an average angle of 2.88° (e.g. Huangliu Formation), a progradation and aggradation phase characterized by low-angle ascending trajectories (e.g., Yinggehai and Lower Ledong Formation), exhibiting an average angle of 3.79°, and aggradational phases characterized by high-angle ascending shelf-edge trajectories (e.g., Upper Ledong Formation), exhibiting an average angle of 30.03°.

The CC' seismic line is located in the eastern part of the QDNB (Figure 5). Similarly, the shelf noticeably narrows here, and the clinoform exhibits chaotic stratigraphy with reduced sediment volume. The clinoform show an aggradation pattern, shelf-edge trajectory is very steep (from Huangliu Fromation to the sea floor), with an average angle of 62.54°.

Significant variations are observed in the trajectory, stack pattern and sedimentary system. A notable feature is the transition from

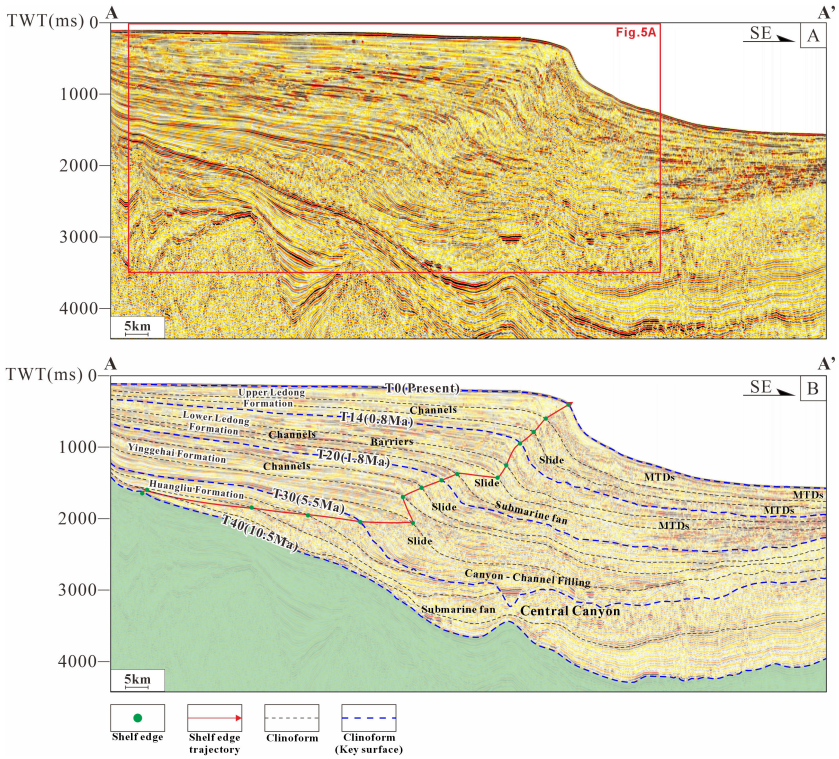

FIGURE 3
Uninterpreted **(A)** and interpreted **(B)** longitudinal (downdip) seismic section AA' in the western part of the Qiongdongnan Basin (see locations in Figure 1B). The shelf edges are marked by red lines and green dots.

10.3389/fmars.2025.1519179

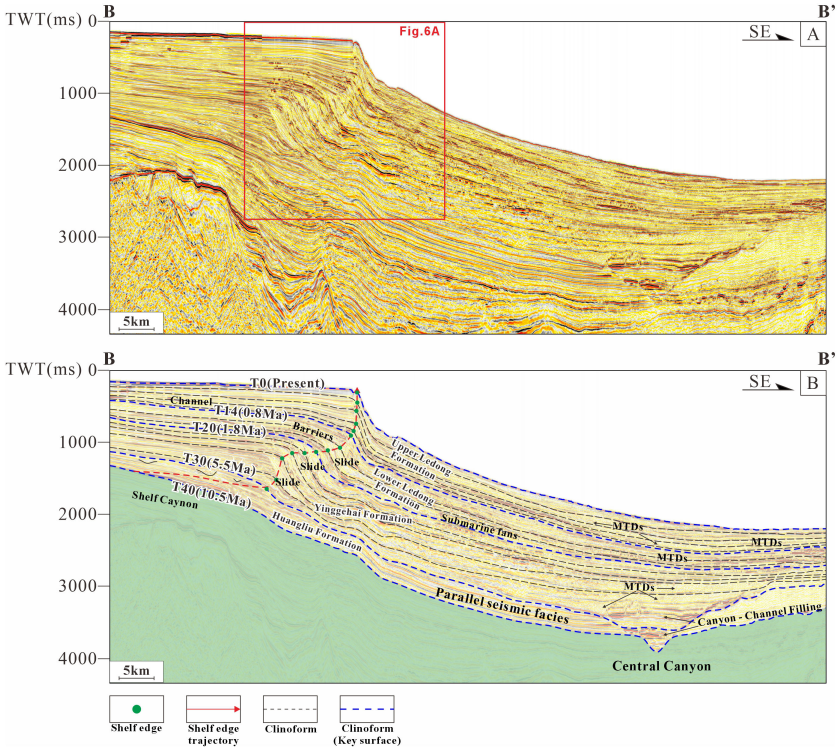

FIGURE 4
Uninterpreted **(A)** and interpreted **(B)** longitudinal (downdip) seismic section BB' in the western part of the Qiongdongnan Basin (see locations in Figure 1B). The shelf edges are marked by red lines and green dots.

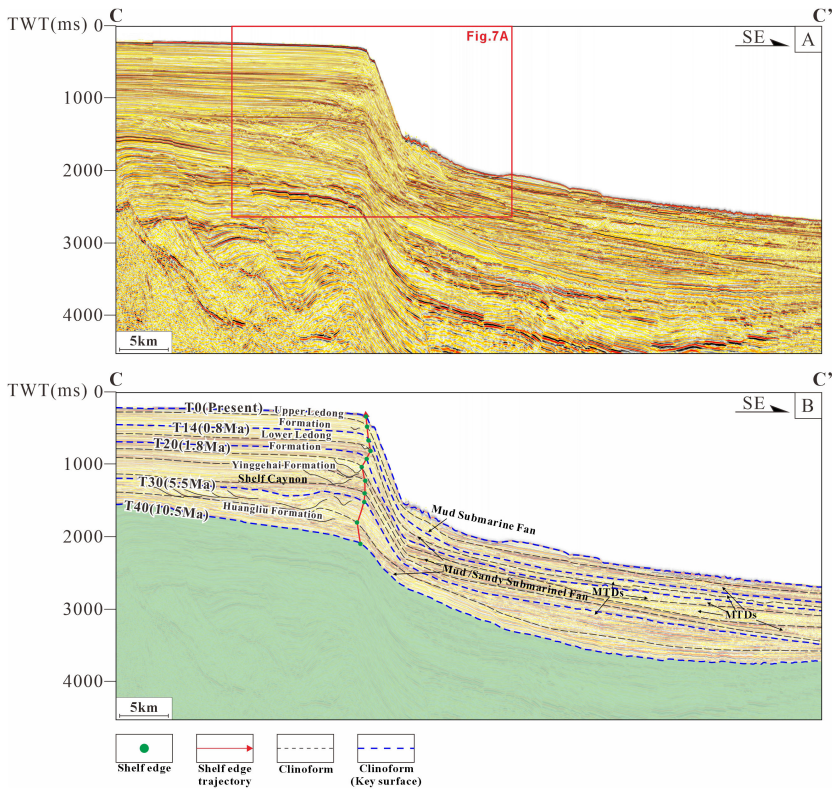

FIGURE 5
Uninterpreted **(A)** and interpreted **(B)** longitudinal (downdip) seismic section CC' in the western part of the Qiongdongnan Basin (see locations in Figure 1B). The shelf edges are marked by red lines and green dots.

dominantly progradation to aggradation in the shelf edge trajectories from west to east. The trajectories in the west are S-shaped and show continuous progradation, whereas those in the east are dominated by aggradation, with steeper and shorter slope trajectories. This significant difference indicates that the growth rate of the western shelf of the QDNB far exceeds that of the eastern shelf. On the basis of shelf growth, progradation and sedimentation rates can be estimated (Table 1), inferring changes in the sediment supply (Figure 6).

4.2 Clinothem types

Three shelf-edge clinothem variations can be identified in the QDNB. O-type (On the Shelf Type) clinothems are characterized by thicker deposits in the topset and thinner deposits in the foreset and bottomset, indicating higher aggradation rates and lower progradation rates on the shelf (Figures 7, 8). The S-Type (Slope Type) clinothems, both the topset and bottomset have relatively thin sedimentary layers compared to the thicker deposits on the foreset (Figures 7, 8). F-type (Basin Floor Type) clinothems, thinner deposits are present in the topset and foreset, but thicker deposits are present in the bottomset (Figures 7–9). This type represents two scenarios: extensive sediment transport to the basin floor, forming a highly progradational clinoform, or slope erosion by the overlying progradational clinoform (Chen et al., 2018).

The three varieties of clinothems are distributed along seismic line AA' (Figure 7): F-type (clinothems 1, 2, 3, 5, 6, and 10), O-type (clinothems 4, 7, and 8), and S-type (clinothems 9, 11-15). During the initial stages of slope development during the deposition of the Huangliu Formation and the Yinggehai Formations, the dominant feature that developed was the forwards-prograding F-type clinothem, which transitioned to O-type or S-type clinothems at the sequence tops. The clinothems along seismic line BB', similar to those along seismic line AA', generally follow an "S-F-O" pattern (Figure 8). During the deposition of Huangliu Formation, the resulting clinothem was the F-type and the O-type, indicating a shift in sediment transport patterns. Seismic line CC' exhibits a distinct distribution pattern of slope morphologies (Figure 9), is dominated by the O-type, with significant sediment accumulation above the shelf and some transport to the basin but minimal preservation of sediments on the slope.

4.3 Sedimentary facies types and characteristics

In the following, the RMS attribute map (Figure 10) in the bottom surface of Lower Ledong Formation (T20) and the variance body slices map (Figure 11) in the bottom surface of Upper Ledong Formation (T14) are taken as examples to introduce the sedimentary facies identification and draw a sedimentary facies map of the study area.

4.3.1 Seismic facies 1-2: shelf-edge delta and sand barriers

Owing to the limitations of the surveyed 3D seismic area, a complete shelf-margin delta system cannot be identified within the study area. The delta system deposits are present mainly at the northernmost end of the surveyed area, and they continuously prograded into the basin (Figure 10). The deposits exhibit moderate to strong amplitudes with sigmoid or oblique seismic reflection characteristics. The shelf-margin delta deposits in the Huangliu Formation study area are large in scale and become progressively smaller towards the Ledong Formation (Figure 12). In the topset layers near the shelf edge, small-scale incised channel sand deposits can be locally observed (Figures 11A, C).

The sand barrier ridges developed mainly in the topset near the shelf edge during deposition of the Ledong Formation. Some moderate- to strong-amplitude, parallel continuous seismic reflections are considered deposits of coastal barrier ridges.

4.3.2 Seismic facies 3: slope fan

Slope fan deposits exhibit distinct morphologies in seismic data. Specifically, these deposits downlop the underlying sediments in the slope direction while thickening towards the basin. They show moderate to high continuity and wedge or trough-shaped reflections in seismic profiles (Figure 13A).

4.3.3 Seismic facies 4: Submarine fan

Submarine fans are located at the basin bottom, adjacent to slope fans. Their deposits display strong, continuous-amplitude reflections, distinct from the continuous weak-amplitude seismic characteristics of the overlying and surrounding submarine mudstones (Figures 13B, D). Turbidite channels are primarily distributed within the basin plains, reflecting the process of the basin receiving gravity flow deposits in a relatively calm environment, characterized seismically by "U"- or "V"-shaped incisions (Figures 13B).

4.3.4 Seismic facies 5: mass transport deposits

Mass transport deposits (MTDs) are crucial components of deep-water sedimentary systems and are characterized by low-amplitude chaotic reflections. The development and distribution of MTDs are influenced by various factors and can be correlated with the varieties of shelf-edge trajectories. Stratigraphically, the phase of early slope development of the Huangliu Formation is characterized by fewer and smaller MTDs. The overlying Yinggehai Formation strata exhibiting an aggradational trend on the slope, leading to the entire basin floor being filled with extensive and thick MTDs, which are noticeably greater in number than the underlying Huangliu Formation. During the deposition of Ledong Formation, owing to periodic fluctuations in sea level, sizable MTDs also developed. Compared with those in the Huangliu Formation phase, the number and scale of MTDs during the deposition of Lower Ledong Formation decreased, then increased during the

10.3389/fmars.2025.1519179

TABLE 1 Progradation and aggradation distance, progradation and aggradation rate and Shelf-edge trajectories in the Miocene -Pleistocene succession of the Qiongdongnan Basin.

Seismic line	Boundraies	Progradation distance (m)	Aggradation distance (m)	Progradation Rate (km/Myr)	Aggradation Rate (km/Myr)	Shelf-edge trajectory (°)
1	T40-T30	32497.18	-43.71	6.50	-0.01	-0.08
	T30-T20	17173.75	601.07	4.64	0.16	2.00
	T20-T14	17670.18	199.61	17.67	0.20	0.65
	T14-T0	17557.35	794.72	21.95	0.99	2.59
2 (Figure 2)	T40-T30	25019.74	-16.26	5.00	0.00	-0.04
	T30-T20	11320.99	572.97	3.06	0.15	2.90
	T20-T14	19937.95	274.32	19.94	0.27	0.79
	T14-T0	13593.46	797.77	16.99	1.00	3.36
3	T30-T20	6966.90	243.82	1.88	0.07	2.00
	T20-T14	10330.01	62.52	10.33	0.06	0.35
	T14-T0	6981.01	855.71	8.73	1.07	6.99
4	T30-T20	7199.14	232.86	1.95	0.06	1.85
	T20-T14	10078.04	84.01	10.08	0.08	0.48
	T14-T0	6236.37	827.47	7.80	1.03	7.56
5	T30-T20	8462.77	246.73	2.29	0.07	1.67
	T20-T14	9623.92	47.34	9.62	0.05	0.28
	T14-T0	6735.61	848.89	8.42	1.06	7.18
6	T30-T20	8431.74	233.51	2.28	0.06	1.59
	T20-T14	13142.16	151.97	13.14	0.15	0.66
	T14-T0	5351.64	710.71	6.69	0.89	7.56
7	T30-T20	6325.69	146.24	1.71	0.04	1.32
	T20-T14	9087.06	106.37	9.09	0.11	0.67
	T14-T0	3553.97	782.13	4.44	0.98	12.41
8	T30-T20	7299.74	125.62	1.97	0.03	0.99
	T20-T14	10188.98	142.75	10.19	0.14	0.80
	T14-T0	3345.24	745.13	4.18	0.93	12.56
9	T30-T20	8469.35	59.54	2.29	0.02	0.40
	T20-T14	7423.84	145.87	7.42	0.15	1.13
	T14-T0	5094.02	642.89	6.37	0.80	7.19
10	T30-T20	6795.79	170.63	1.84	0.05	1.44
	T20-T14	9295.79	187.12	9.30	0.19	1.15
	T14-T0	3931.93	658.72	4.91	0.82	9.51
11	T30-T20	6729.03	211.73	1.82	0.06	1.80
	T20-T14	9105.87	224.15	9.11	0.22	1.41
	T14-T0	2158.71	576.23	2.70	0.72	14.95
12	T30-T20	5311.21	89.09	1.44	0.02	0.96
	T20-T14	8529.52	360.22	8.53	0.36	2.42
	T14-T0	453.18	470.37	0.57	0.59	46.07

(Continued)

10.3389/fmars.2025.1519179

TABLE 1 Continued

Seismic line	Boundraies	Progradation distance (m)	Aggradation distance (m)	Progradation Rate (km/Myr)	Aggradation Rate (km/Myr)	Shelf-edge trajectory (°)
13	T30-T20	7841.29	454.98	2.12	0.12	3.32
	T20-T14	7865.74	249.56	7.87	0.25	1.82
	T14-T0	1669.80	502.17	2.09	0.63	16.74
14	T30-T20	6720.57	436.39	1.82	0.12	3.72
	T20-T14	5635.58	363.12	5.64	0.36	3.69
	T14-T0	2179.39	431.74	2.72	0.54	11.21
15 (Figure 3)	T30-T20	6972.55	462.09	1.88	0.12	3.79
	T20-T14	4449.98	223.78	4.45	0.22	2.88
	T14-T0	948.66	548.28	1.19	0.69	30.03
16	T30-T20	4266.64	311.50	1.15	0.08	4.18
	T20-T14	4089.88	78.56	4.09	0.08	1.10
	T14-T0	4321.17	653.85	5.40	0.82	8.60
17	T30-T20	7444.53	461.51	2.01	0.12	3.55
	T20-T14	5550.02	37.76	5.55	0.04	0.39
	T14-T0	1839.04	607.24	2.30	0.76	18.27
18	T30-T20	5466.34	373.07	1.48	0.10	3.90
	T20-T14	3901.84	155.39	3.90	0.16	2.28
	T14-T0	1506.21	464.34	1.88	0.58	17.13
19	T30-T20	5688.23	472.55	1.54	0.13	4.75
	T20-T14	3386.61	21.13	3.39	0.02	0.36
	T14-T0	1546.63	190.46	1.93	0.24	7.02
20	T30-T20	4127.49	784.26	1.12	0.21	10.76
	T20-T14	2590.26	403.42	2.59	0.40	8.85
	T14-T0	787.89	438.57	0.98	0.55	29.10
21	T30-T20	3517.30	610.22	0.95	0.16	9.84
	T20-T14	287.70	343.01	0.29	0.34	50.01
	T14-T0	678.83	330.01	0.85	0.41	25.93
22	T40-T30	962.77	544.94	0.19	0.11	29.51
	T30-T20	512.41	627.35	0.14	0.17	50.76
	T20-T14	256.68	277.15	0.26	0.28	47.20
	T14-T0	22.56	191.55	0.03	0.24	83.28
23	T40-T30	481.38	607.24	0.10	0.12	51.59
	T30-T20	652.50	399.07	0.18	0.11	31.45
	T20-T14	95.90	348.89	0.10	0.35	74.63
	T14-T0	-437.19	338.44	-0.55	0.42	-37.74
24 (Figure 4)	T40-T30	242.57	455.41	0.05	0.09	61.96
	T30-T20	218.13	410.76	0.06	0.11	62.03
	T20-T14	98.72	290.15	0.10	0.29	71.21

(Continued)

TABLE 1 Continued

Seismic line	Boundraies	Progradation distance (m)	Aggradation distance (m)	Progradation Rate (km/Myr)	Aggradation Rate (km/Myr)	Shelf-edge trajectory (°)
	T14-T0	271.72	387.52	0.34	0.48	54.96
25	T40-T30	342.23	619.29	0.07	0.12	61.07
	T30-T20	1004.14	638.03	0.27	0.17	32.43
	T20-T14	92.14	229.52	0.09	0.23	68.13
	T14-T0	-30.09	128.23	-0.04	0.16	-76.80
26	T40-T30	86.50	539.64	0.02	0.11	80.89
	T30-T20	483.26	511.61	0.13	0.14	46.63
	T20-T14	-198.38	223.49	-0.20	0.22	-48.41
	T14-T0	-136.33	140.86	-0.17	0.18	-45.94

deposition of Upper Ledong Formation. Spatially, MTDs typically show a pattern of fewer and smaller deposits in the west and more extensive deposits in the east.

MTDs extensively develop in basins and are characterized seismically by chaotic amplitudes and poor continuity (Wang et al., 2013; Cheng et al., 2021). For the variance attributes, MTDs correspond to higher variance values, representing a set of irregular and darker-coloured sediments (Figures 11, 13A, B). Muddy channels seismically exhibit extremely strong incision capabilities (Figures 14C, D), and variance attribute slices reveal channel-like deposits with high variance values in the deep-sea plane.

4.4 Evolution of the sedimentary system

4.4.1 Huangliu formation

Since the late Miocene, the subsidence centre of the southeastern QDNB has continuously shifted southwards, giving the basin a topography that is relatively high in the west and relatively low in the east (Figure 12A). This feature, which was recorded in the late Miocene and Pliocene, influenced the sedimentary fill. During the late Miocene, shelf deltas developed above the shelf, delivering large amounts of clastic materials to the deep-water areas of the southeastern QDNB. The long-term stable sediment transport provided the conditions for the extensive development of the shelf, which supplied sediment into the basin to form submarine fans. In the eastern part of the study area, mass transport deposits (MTDs) are present, are oriented along the trend of the sedimentary strata and formed below the slope in the deep-sea plain area. During this period, the iconic Central Canyon of the southeastern Qiong Basin began to take shape, extending in the SW–NE direction, and was primarily filled with sandy turbidite channels. The MTDs filling the east side of the Central Canyon are considered to have been influenced by the northern slope's contribution to the canyon's infill.

4.4.2 Yinggehai formation

This period was marked by multiple phases of large-scale, thick mass transport deposits (MTDs), which had a broader distribution than the Central Canyon did, spanning almost the entire study area (Figure 12B). The shelf deltas, with canyons near the shelf edge, exhibited some continuity but were reduced in scale and number compared with those in the late Miocene. By end Yinggehai Formation time, submarine fans and MTDs alternated at the base of the bottomset, with the overall trend showing a greater quantity of slope sands in the western part of the study area than in the

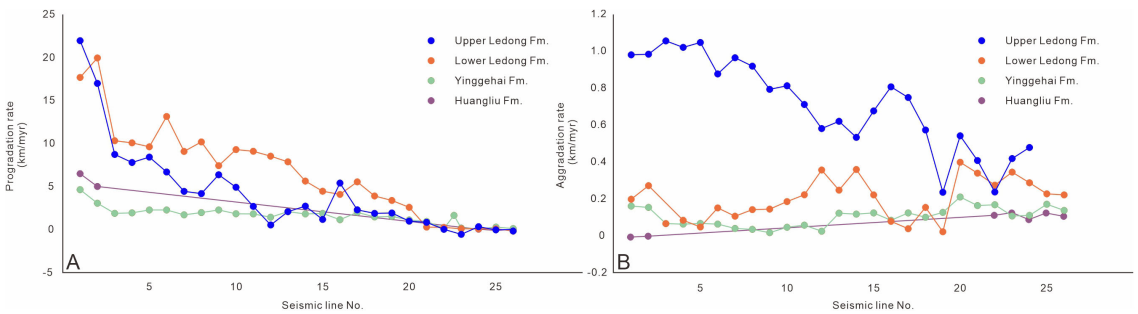

FIGURE 6
Growth rate of the shelf margin. Progradation **(A)** and aggradation **(B)** rates for each seismic line. Note that from older to younger sequences, the progradation and aggradation rates increase from west (No. 1 section) to east (No. 26 section). The seismic sections in Figures 2–4 correspond to the No. 2, No. 15 and No. 24 seismic sections, respectively.

10.3389/fmars.2025.1519179

eastern part, whereas the MTDs in the eastern part were larger and thicker than those in the western part.

4.4.3 Lower ledong formation

By the early Pleistocene, deltas on the shelf in the study area had decreased in size compared with those in the late Miocene–Pliocene; only a small number of shelf delta facies were observable within the surveyed 3D seismic area and the area of shelf sand ridges (Figure 12C). Channels on the slope were extensively developed, and the presence of slumps indicated an increased sedimentation rate. The cooler Pleistocene climate led to extensive progradation in the western part of the QDNB in the early Pleistocene, providing sediment for the formation of slope fans and submarine fans. Concurrently, with the periodic fluctuations in sea level, normal sedimentation and mass transport deposits overlapped. The sedimentary system in the eastern part of the basin showed some continuity, which was related to the inherited configuration of the shelf edge. Channels on the shelf became less frequent than those in the underlying strata, but those on the slope increased in size, with the basin developing medium-amplitude mixed sand–mud submarine fans. The frequency and scale of mass transport events also significantly increased.

4.4.4 Upper ledong formation

From the middle Pleistocene to the present, the configuration of the shelf-edge trajectories and the development of sedimentary systems differed from those of the underlying strata (Figure 12D). The internal shelf edge strata of the basin exhibited a rapidly

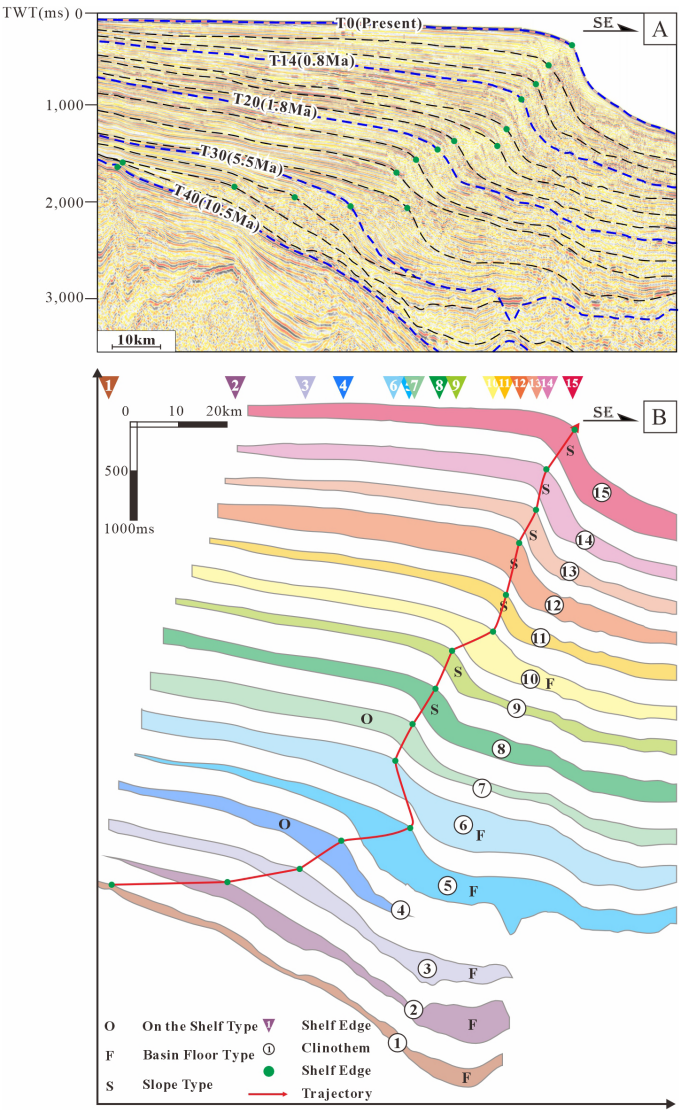

FIGURE 7
Patterns of the shapes of clinothem sets **(B)** from the seismic section **(A)** shown in Figure 2. F-F-type (Basin Floor Type) clinothems; S-S-type (Slope Type) clinothems; O-O-type (On the Shelf Type) clinothems.

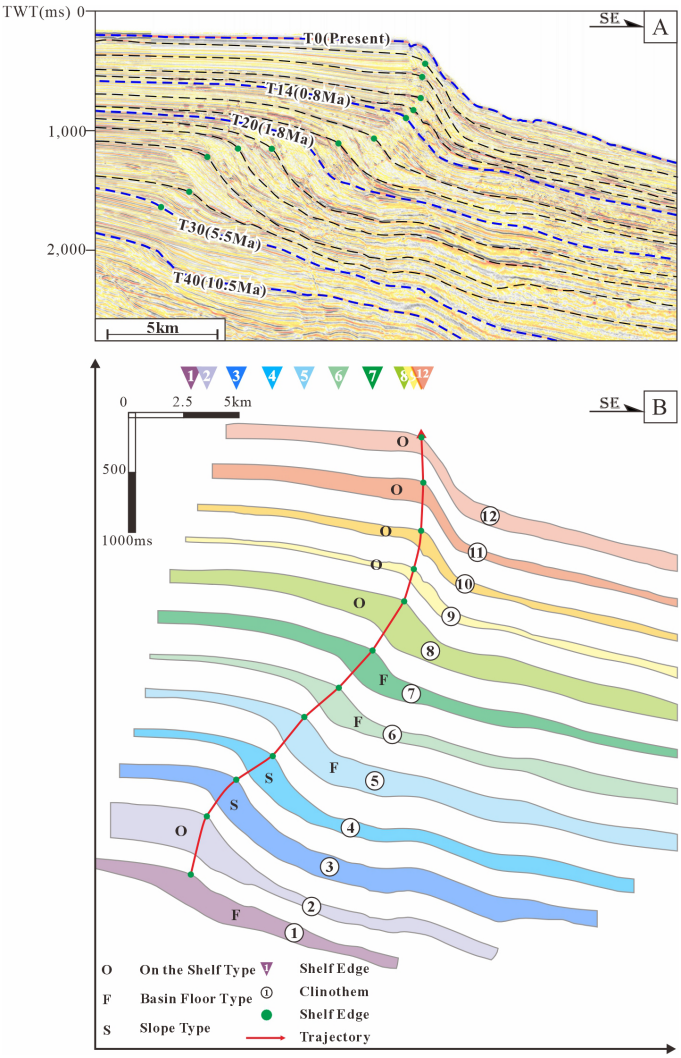

FIGURE 8
Patterns of the clinothem sets **(B)** from the seismic section **(A)** shown in Figure 3. F-F-type (Basin Floor Type) clinothems; S-S-type (Slope Type) clinothems; O-O-type (On the Shelf Type) clinothems.

aggrading stacking pattern overall. High sedimentation rates, high accommodation space, and fewer channels resulted in fewer sandy submarine fans developing, and more mixed sand-mud/mud-rich submarine fans developed. At the same time, periodic fluctuations in the relative sea level responded to Pleistocene climatic transitions, making it difficult for sediments to accumulate on the shelf, thereby resulting in the development of large-scale, multiphase mass transport depositional systems within the basin.

5 Discussion

5.1 Clinothem patterns and deep-water sedimentary development

In general terms, there may be a relationship between different shelf-edge trajectories, stacking patterns and related sedimentary systems at different location of the sedimentary basin. In other words, clinothems is an effective predictor of sedimentary systems (Liu et al., 2007; Surlyk and Larsen, 2023). The growth stage of the submarine fans in the Washakie Basin is closely related to the contemporaneous changes of the shelf-edge trajectories (Koo et al., 2016), the development of sheet sands and MTDs in the Northern Carnarvon Basin are also controlled by the shelf-margin architecture (Paumard et al., 2018), the types and development scale of the sedimentary system are also related to the clinothem pattern (Shepherd et al., 2024). Therefore, Changes in clinothem pattern can reasonably reflect the efficiency of sediment transport to deep waters (Carvajal and Steel, 2006, Carvajal and Steel, 2009; Covault and Graham, 2010; Anell et al., 2014; Gong et al., 2016b; Pellegrini et al., 2018; Gong et al., 2019a).

At the shelf edge of the western QDNB, there were phases of strong progradational clinoforms during the Huangliu Formation sedimentary period, a coupling of strong aggradational and progradational clinoforms during the Yinggehai Formation sedimentary period, and strong progradational clinoforms during the Lower Ledong Formation sedimentary period, followed by

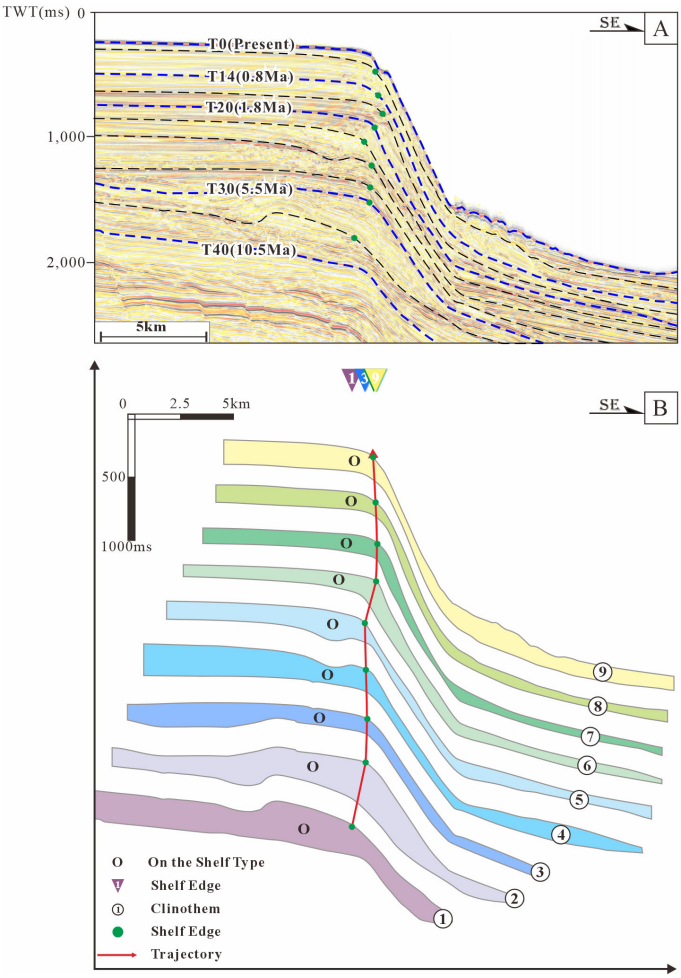

FIGURE 9
Patterns of shapes of clinothem sets **(B)** from the seismic section **(A)** shown in Figure 4. O-O-type (On the Shelf Type) clinothems.

strong aggradational clinothems in the Upper Ledong Formation sedimentary period.

In the western part of the study area, the development of the shelf edge is more likely due to a supply-dominated system. Clinoforms with strong progradation indicate the ability to transport sediments to farther basin floors (Figure 15A), whereas those with strong aggradation are more likely to be associated with sediment sliding, landslides, or MTDs (Figure 15B). Notably, since the Pliocene–Pleistocene, there has been a continuous increase in sediment supply, with higher sedimentation rates and finer grained sediments in the Upper Ledong Formation. The development of O-type clinothems in the early Pleistocene appears to be related not only to accommodation space and sediment supply but also possibly to the rapid accumulation of fine-grained sediments on slopes. When the slope gradient exceeds a certain threshold, the slope collapses (mud-rich slopes are more prone to collapse than are sand-rich slopes; Anell and Midtkandal, 2017; Wolinsky and Pratson, 2007). This is also the reason for the increased development of slump bodies on slopes during the deposition of Ledong Formation and mass transport deposits (MTDs) within the basin. In contrast, the shelf-edge trajectories in the eastern part of the study area are entirely different and are dominated by strong aggradation of the clinothem and frequent occurrences of sliding and slumping bodies. Typically, strong aggradational clinothems are not conducive to the formation of deep-water sands (Sztanó et al., 2013; Gong et al., 2019b), indicating a different deep-water sediment transport mode (Figure 15C). Tectonic activity may be another significant factor influencing the development and distribution of deep-water sediments. Faults often lead to changes in local topography, which become preferred pathways for sediment transport (Harris and Whiteway, 2011; Fisher et al., 2021). The observed submarine canyons perpendicular to the shelf edge are considered products of shelf fault evolution (He et al., 2013). Recent research indicates that deep-water sands that developed in strong aggradational clinothems are closely related to these canyons (Cerrillo-Escoriza et al., 2024; Huang et al., 2024).

5.2 Factors controlling clinothem patterns

Clinothems are prism-shaped deposits that form during the transport of sediments from the basin margin platform and are

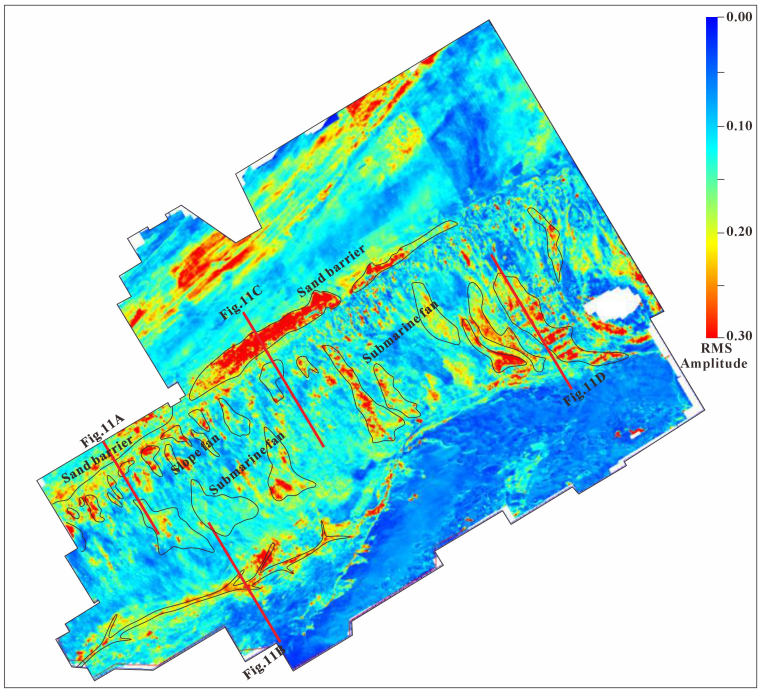

FIGURE 10
RMS amplitude map of the Qiongdongnan Basin (20 ms (twt) window below the T20 surface).

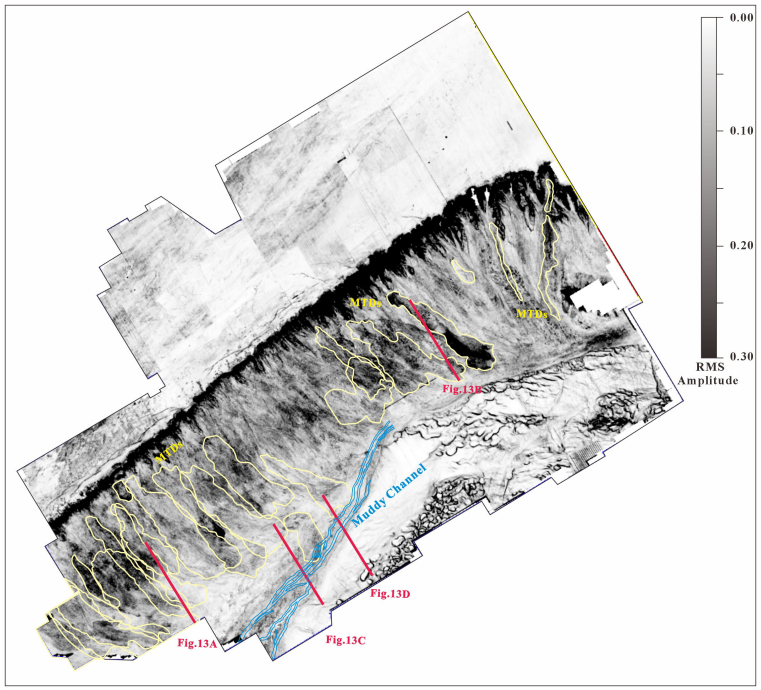

FIGURE 11
Variance slice map of the Qiongdongnan Basin (20 ms (twt) window below the T20 surface).

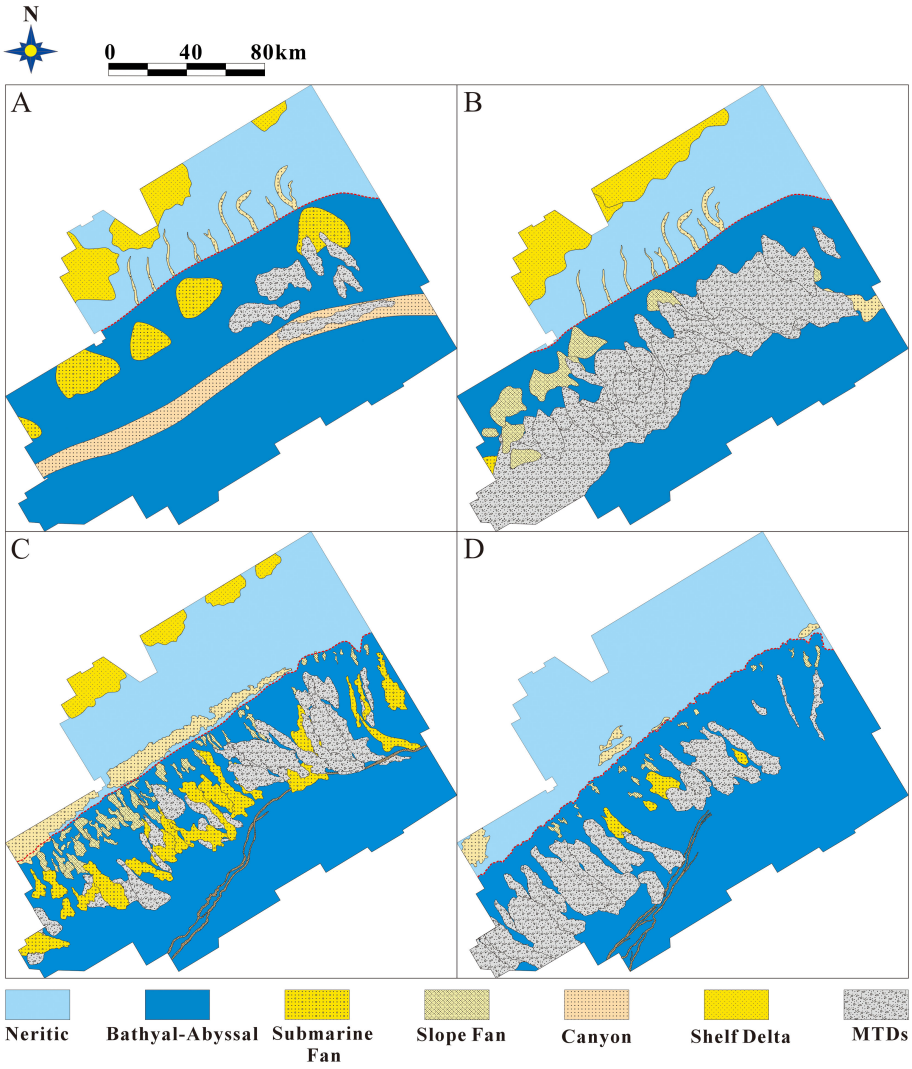

FIGURE 12
Mio–Pleistocene sedimentary facies map. **(A)** Sedimentary facies map of the Huangliu Formation. **(B)** Sedimentary facies map of the Yinggehai Formation. **(C)** Sedimentary facies map of the Lower Ledong Formation. **(D)** Sedimentary facies map of the Upper Ledong Formation.

influenced by the sediment supply and relative sea-level changes (Pellegrini et al., 2020). With rising relative sea levels, a flooding surface forms, leading to the creation of clinothem through continuous progradation or aggradation (Shepherd et al., 2023). Conversely, during relative sea level fall, shallow-water shelf environments develop, and existing shelf sediments undergo truncation or erosion (Gong et al., 2016b).

Over time, ongoing sediment progradation and aggradation results in various growth patterns of the shelf edge and clinothem (Cosgrove et al., 2020; Pellegrini et al., 2020). These clinothems are differentiated mainly on the basis of changes in thickness across the shelf-margin architecture and stacking patterns (Chen et al., 2018; Anell, 2024). Within a sequence, sediment layers on the slope develop and vary longitudinally (Paumard et al., 2020; Dafoe et al., 2023). The relationship between changes in base-level and sediment supply influences variations in water depth, along with the erosion and movement of shelf edges (Johannessen and Steel, 2005; Catuneanu et al., 2009; Anell and Midtkandal, 2017), leading to the development of various types of shelf margin trajectories and clinothems (Hampson and Storms, 2003; Pellegrini et al., 2018; Ramon-Duenas et al., 2018) (Figure 16A). In this process, the progradation, aggradation, and retrogradation at the shelf edge delineate continually rising, falling, and stable shelf margin trajectories (Hampson and Storms, 2003; Helland-Hansen and Hampson, 2009; Gauchery et al., 2021). These different trajectories can be utilized to reconstruct various depositional environments, and at a minimum, they allow shelf edge responses to controlling factors, such as accommodation space, relative sea level, and sedimentation rate during different periods, to be inferred (Anell et al., 2014; Pellegrini et al., 2018).

An uneven sediment distribution can cause variations in relief and long-term accretion patterns across different margin sectors (Zhao et al., 2019; Zhuo et al., 2019). The formation of clinothems takes place within the framework of third-order sequences, where patterns of clinothems are governed by changes in relative sea level and sediment supply (Chen et al., 2020). During periods of rapid sea-level rise, the majority of sediments are unable to pass beyond the

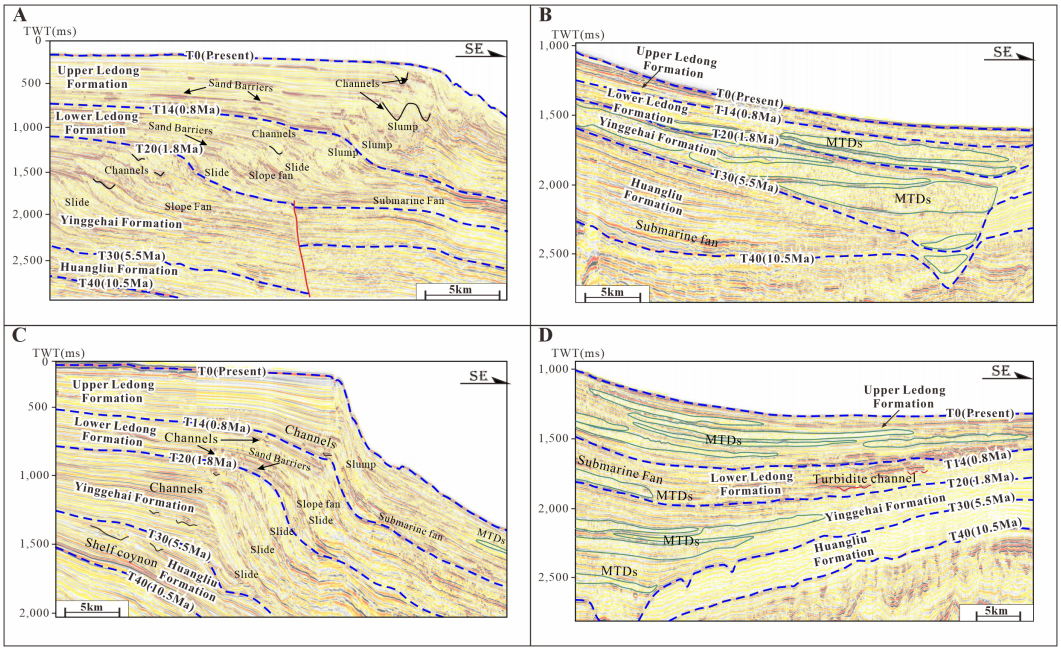

FIGURE 13
(A–D) Seismic sections of the west to east slope and basin plane area of the Qiongdongnan Basin.

shelf edge and remain restricted to the shelf. Typically, the topset are well preserved, but bottomset are less developed, with high sedimentation rates leading to thick topset. The clinothems that developed during this phase are O-type clinothems were dominated by aggradation, where the thickest topset accumulate near the shelf edge, making it difficult to bypass the shelf (Figure 16B). F-type clinothems usually form when the accommodation space is limited. During this phase, the base-level cycle shows a declining trend (Figure 16C). As sediment continues to accumulate and with limited accommodation space on the topset, sediments are forced to bypass the shelf and be deposited on the foreset and bottomset. Flat or declining shelf margin trajectories are usually associated with this type of clinothem (Chen et al., 2018). During a complete S-type clinothem sedimentation period, there was a coupling of deposition

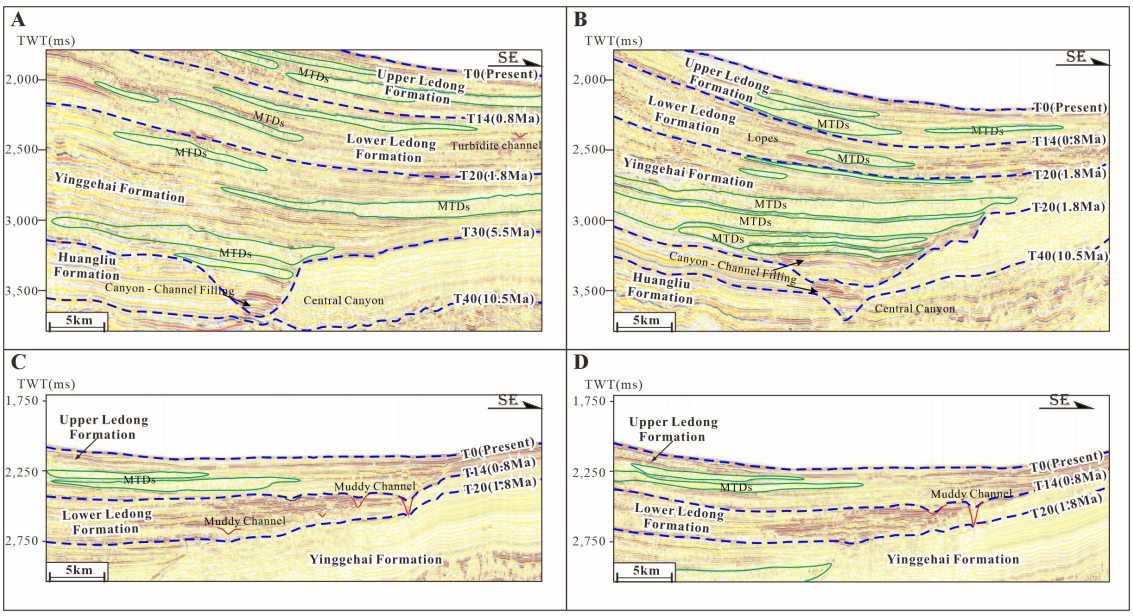

FIGURE 14
(A–D) Seismic sections of the west to east slope and basin plane area of the Qiongdongnan Basin.

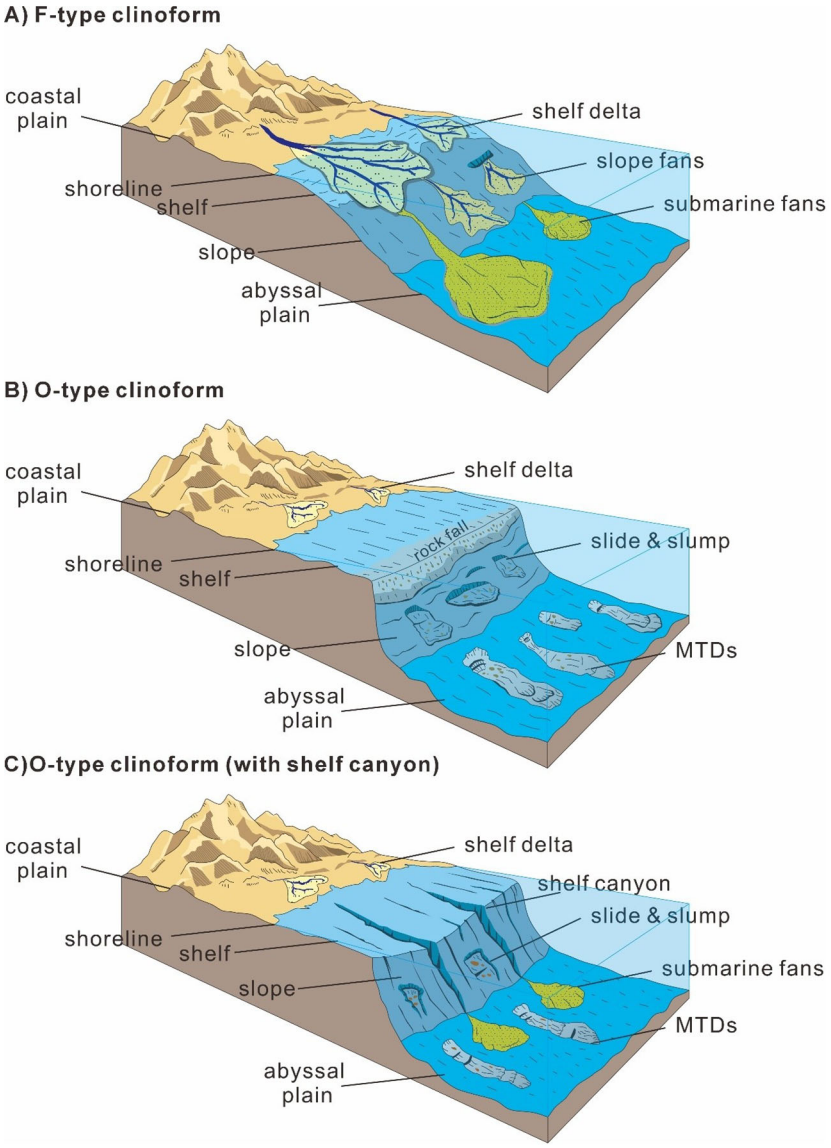

FIGURE 15
(A) In the area of F-type clinothem development, sediments are transported from the shelf to the basin plain and deposited on the slope to form slope fans and on the basin floor to form submarine fans. **(B)** In the area of O-type clinothem development, sediments tend to accumulate on the shelf, slumps form on the slope, and MTDs form on the basin plain. **(C)** In the area of O-type clinothem (with shelf canyon) development, sediments tend to accumulate on the shelf. Some of the sediments are transported to the abyssal plain through shelf canyons and deposited to form submarine fans, slumps form on the slope, and MTDs form on the basin plain.

and progradation related to water level fluctuations and sediment supply (Figure 16D). S-type clinothems typically develop during stages of continuous sea-level rise and abundant sediment supply, corresponding to two similar periods. During the early stages of sea-level rise, sediments are easily deposited on the topset or foreset, making it more difficult to transport them into the basin. During increasing in accomodation periods, the increase in accommodation space exceeds the sediment supply, but as the rate of increase slows, the accommodation space gradually decreases, allowing some sediments to bypass the shelf, but they tend to accumulate on the foreset (Sztanó et al., 2013; Gomis-Cartesio et al., 2018).

5.3 Significance for hydrocarbon exploration

With the advancement of oil and gas exploration technologies and the continuous increase in energy demand, the exploration focus has shifted from onshore to deepwater, from the continental shelf to the slope, and even to the basin floor. Submarine fans below the continental shelf edge seem promising for hydrocarbon reservoirs (Gao et al., 2020; Cox et al., 2021; Zhang et al., 2021). This is also the case in the current study area, where deepwater submarine fan sand bodies influenced by the continental shelf edge are the focus of research.

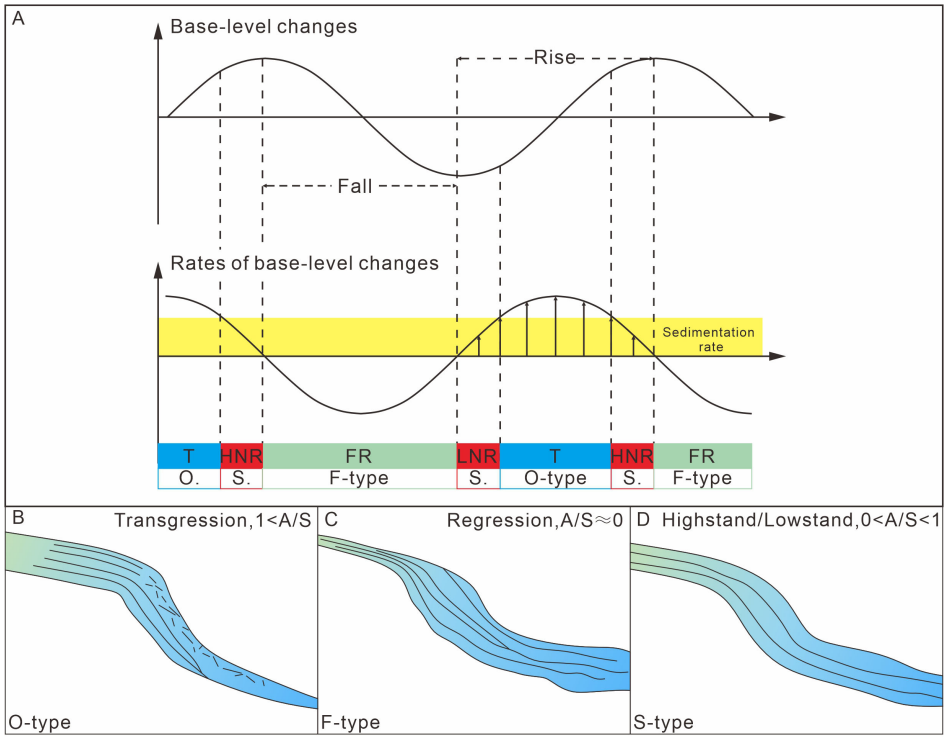

FIGURE 16
Relationships between the base level and clinothem types. **(A)** Concepts of transgression, normal regression and forced regression as defined by the balance between base-level fluctuations and sediment supply (modified after Catuneanu et al., 2009). T, transgression; HNR, highstand normal regression; FR, forced regression; LNR, lowstand normal regression. **(B)** O-type clinothems corresponding to accommodation and supply. **(C)** F-type clinothems corresponding to accommodation and supply. **(D)** S-type clinothems corresponding to accommodation and supply.

Areas where the shelf-edge trajectory decreases or shows a low-angle rise or where F-type clinothems and shelf canyons develop O-type clinothems are the most promising for oil and gas reservoirs. Conversely, areas with a high-angle rising shelf trajectory and developed O-type clinothems may represent potential seal layers. Regions where MTDs and submarine fans overlap may be favourable areas for oil and gas exploration.

6 Conclusions

On the basis of 2D and 3D seismic data, we identified differences between the shelf-edge configuration of the Qiongdongnan Basin and the sedimentary systems of its deep-water areas. The research results in three primary conclusions.

1. Various types of shelf-edge trajectories have been identified within the Mio–Pleistocene sequence of the Qiongdongnan Basin (QDNB). There are three types of clinothems: F-type clinothems, characterized by a more developed bottomset; O-types, characterized by a more developed topset; and S-types, characterized by a more developed foreset.
2. The shelf-edge trajectories and clinothems are controlled by the base level and sediment supply. During periods of rapid relative sea-level rise, the majority of sediments are unable to pass beyond the shelf edge and remain restricted to the shelf. The O-type clinothems with strong aggradation and weak progradation developed during this phase. F-type clinothems are usually formed when the accommodation space is limited. During this phase, the accomodation shows a declining trend. S-type clinothems typically develop during stages of continuous sea-level rise and abundant sediment supply.
3. There is a certain correlation between the development of clinothems and deep-water sedimentary systems. When the shelf trajectory decreases or has a low angle, F-type clinothems are easily formed. In this case, a large amount of sediment is transported to the basin plain. Therefore, during the deposition of the Huangliu Formation and the Lower Ledong Formation, submarine fans developed in the basin plain. When the shelf trajectory is high-angle and increasing, O-type clinothems are most likely to develop. In this case, sediment primarily accumulates on the shelf. Therefore, during the deposition of the Yinggehai Formation and the Upper Ledong Formation, slope failures were prone to occur, leading to the development of MTDs in the basin plain. Additionally, in areas where shelf canyons are widely developed, although O-type clinothems developed, sediment can still be transported to the seafloor through shelf canyons, leading to the development of submarine fans in the basin plain. When submarine fans and MTDs overlap spatially, they can serve

as reservoir-seal combinations, with certain prospects for oil and gas exploration.

Data availability statement

The datasets presented in this study can be found in online repositories. The names of the repository/repositories and accession number(s) can be found in the article/supplementary material.

Author contributions

TL: Conceptualization, Data curation, Methodology, Writing – original draft. DY: Investigation, Methodology, Supervision, Validation, Visualization, Writing – review & editing. EL: Data curation, Project administration, Resources, Writing – review & editing. JZ: Writing – review & editing. XW: Investigation, Supervision, Writing – review & editing. ZL: Writing – review & editing. XL: Writing – review & editing.

Funding

The author(s) declare financial support was received for the research, authorship, and/or publication of this article. This research was supported by the Natural Science Foundation of China (41690131) and National Natural Science Foundation of China (42072142).

Acknowledgments

This research was supported by the Natural Science Foundation of China (41690131) and National Natural Science Foundation of China (42072142).

Conflict of interest

The authors declare that the research was conducted in the absence of any commercial or financial relationships that could be construed as a potential conflict of interest.

Generative AI statement

The author(s) declare that no Generative AI was used in the creation of this manuscript

Publisher's note

All claims expressed in this article are solely those of the authors and do not necessarily represent those of their affiliated organizations, or those of the publisher, the editors and the reviewers. Any product that may be evaluated in this article, or claim that may be made by its manufacturer, is not guaranteed or endorsed by the publisher.

References

Anell, I. (2024). The quintessential s-shape in sedimentology: A review on the formation and controls of clinoform shape. *Earth-Science Rev.* 254, 104821. doi: 10.1016/j.earscirev.2024.104821

Anell, I., and Midtkandal, I. (2017). The quantifiable clinothem – types, shapes and geometric relationships in the Plio-Pleistocene Giant Foresets Formation, Taranaki Basin, New Zealand. *Basin Res.* 29, 277–297. doi: 10.1111/bre.12149

Anell, I., Midtkandal, I., and Braathen, A. (2014). Trajectory analysis and inferences on geometric relationships of an Early Triassic prograding clinoform succession on the northern Barents Shelf. *Mar. Petroleum Geol.* 54, 167–179. doi: 10.1016/j.marpetgeo.2014.03.005

Bauch, D., Cherniavskaia, E., and Timokhov, L. (2016). Shelf basin exchange along the Siberian continental margin: Modification of Atlantic Water and Lower Halocline Water. *Deep Sea Res. Part I: Oceanographic Res. Papers* 115, 188–198. doi: 10.1016/j.dsr.2016.06.008

Browning, J. V., Miller, K. G., Sugarman, P. J., Barron, J., McCarthy, F. M. G., Kulhanek, D. K., et al. (2013). Chronology of Eocene–Miocene sequences on the New Jersey shallow shelf: Implications for regional, interregional, and global correlations. *Geosphere* 9, 1434–1456. doi: 10.1130/GES00857.1

Bryn, B. K. L., Ahokas, J., Patruno, S., Schjelderup, S., Hinna, C., Lowrey, C., et al. (2020). Exploring the reservoir potential of Lower Cretaceous Clinoforms in the Fingerdjupet Subbasin, Norwegian Barents Sea. *Basin Res.* 32, 332–347. doi: 10.1111/bre.12407

Carvajal, C., and Steel, R. (2009). Shelf-edge architecture and bypass of sand to deep water: influence of shelf-edge processes, sea level, and sediment supply. *J. Sedimentary Res.* 79, 652–672. doi: 10.2110/jsr.2009.074

Carvajal, C. R., and Steel, R. J. (2006). Thick turbidite successions from supply-dominated shelves during sea-level highstand. *Geol* 34, 665. doi: 10.1130/G22505.1

Catuneanu, O., Abreu, V., Bhattacharya, J. P., Blum, M. D., Dalrymple, R. W., Eriksson, P. G., et al. (2009). Towards the standardization of sequence stratigraphy. *Earth-Science Rev.* 92, 1–33. doi: 10.1016/j.earscirev.2008.10.003

Cerrillo-Escoriza, J., Lobo, F. J., Puga-Bernabéu, Á., Bárcenas, P., Mendes, I., Pérez-Asensio, J. N., et al. (2024). Variable downcanyon morphology controlling the recent activity of shelf-incised submarine canyons (alboran sea, western Mediterranean). *Geomorphology* 453, 109127. doi: 10.1016/j.geomorph.2024.109127

Chen, S., Steel, R., Olariu, C., and Li, S. (2018). Growth of the paleo-Orinoco shelf-margin prism: Process regimes, delta evolution, and sediment budget beyond the shelf edge. *GSA Bull.* 130, 35–63. doi: 10.1130/B31553.1

Chen, S., Steel, R., Wang, H., Zhao, R., and Olariu, C. (2020). Clinoform growth and sediment flux into late Cenozoic Qiongdongnan shelf margin, South China Sea. *Basin Res.* 32, 302–319. doi: 10.1111/bre.12400

Cheng, C., Jiang, T., Kuang, Z., Lai, H., Liang, J., Ren, J., et al. (2023). Sand-rich Pleistocene deep-water channels and their implications for gas hydrate accumulation: Evidence from the Qiongdongnan Basin, northern South China Sea. *Deep Sea Res. Part I: Oceanographic Res. Papers* 198, 104101. doi: 10.1016/j.dsr.2023.104101

Cheng, C., Jiang, T., Kuang, Z., Ren, J., Liang, J., Lai, H., et al. (2021). Seismic characteristics and distributions of quaternary mass transport deposits in the qiongdongnan basin, northern south China sea. *Mar. Pet. Geol.* 129, 105118. doi: 10.1016/j.marpetgeo.2021.105118

Clift, P. D., and Sun, Z. (2006). The sedimentary and tectonic evolution of the Yinggehai–Song Hong basin and the southern Hainan margin, South China Sea: Implications for Tibetan uplift and monsoon intensification. *J. Geophysical Research: Solid Earth* 111 (B6). doi: 10.1029/2005JB004048

Cosgrove, G. I. E., Poyatos-Moré, M., Lee, D. R., Hodgson, D. M., McCaffrey, W. D., and Mountney, N. P. (2020). Intra-clinothem variability in sedimentary texture and process regime recorded down slope profiles. *Sedimentology* 67, 431–456. doi: 10.1111/sed.12648

Covault, J. A., and Graham, S. A. (2010). Submarine fans at all sea-level stands: Tectono-morphologic and climatic controls on terrigenous sediment delivery to the deep sea. *Geology* 38, 939–942. doi: 10.1130/G31081.1

Cox, D. R., Huuse, M., Newton, A. M., Sarkar, A. D., and Knutz, P. C. (2021). Shallow gas and gas hydrate occurrences on the northwest Greenland shelf margin. *Mar. Geology* 432, 106382. doi: 10.1016/j.margeo.2020.106382

Dafoe, L. T., Dickie, K., and Williams, G. L. (2023). An integrated clinoform trajectory and sequence stratigraphic model for the Labrador margin, offshore eastern Canada. *Mar. Petroleum Geology* 155, 106310. doi: 10.1016/j.marpetgeo.2023.106310

Fisher, W. L., Galloway, W. E., Steel, R. J., Olariu, C., Kerans, C., and Mohrig, D. (2021). Deep-water depositional systems supplied by shelf-incising submarine canyons: Recognition and significance in the geologic record. *Earth-Science Rev.* 214, 103531. doi: 10.1016/j.earscirev.2021.103531

Gamberi, F., Pellegrini, C., Dalla Valle, G., Scarponi, D., Bohacs, K., and Trincardi, F. (2020). Compound and hybrid clinothems of the last lowstand Mid-Adriatic Deep: Processes, depositional environments, controls and implications for stratigraphic analysis of prograding systems. *Basin Res.* 32, 363–377. doi: 10.1111/bre.12417

Gao, M., Xu, S., Zhuo, H., Wang, Y., and Wu, S. (2020). Coupling relationship between shelf-edge trajectories and slope morphology and its implications for deep-water oil and gas exploration: A case study from the passive continental margin, East Africa. *J. Earth Sci.* 31, 820–833. doi: 10.1007/s12583-020-1288-8

Gauchery, T., Rovere, M., Pellegrini, C., Cattaneo, A., Campiani, E., and Trincardi, F. (2021). Factors controlling margin instability during the Plio-Quaternary in the Gela Basin (Strait of Sicily, Mediterranean Sea). *Mar. Petroleum Geology* 123, 104767. doi: 10.1016/j.marpetgeo.2020.104767

Gomis-Cartesio, L. E., Poyatos-Moré, M., Hodgson, D. M., and Flint, S. S. (2018). Shelf-margin clinothem progradation, degradation and readjustment: Tanqua depocentre, Karoo Basin (South Africa). *Sedimentology* 65, 809–841. doi: 10.1111/sed.12406

Gong, Z., and Li, S. (1997). *Basin Analysis and Petroleum Accumulation of the Northern South China Sea Continental Margin Basin*. (Beijing: Science Press). (In Chinese with English abstract).

Gong, C., Qi, K., Ma, Y., Li, D., Feng, N., and Xu, H. (2019a). Tight coupling between the cyclicity of deep-water systems and rising-then-flat shelf-edge pairs along the submarine segment of the Qiongdongnan sediment-routing system. *J. Sedimentary Res.* 89, 956–975. doi: 10.2110/jsr.2019.47

Gong, C., Steel, R. J., Wang, Y., Lin, C., and Olariu, C. (2016a). Grain size and transport regime at shelf edge as fundamental controls on delivery of shelf-edge sands to deepwater. *Earth-Science Rev.* 157, 32–60. doi: 10.1016/j.earscirev.2016.04.002

Gong, C., Steel, R. J., Wang, Y., Lin, C., and Olariu, C. (2016b). Shelf-margin architecture variability and its role in sediment-budget partitioning into deep-water areas. *Earth-Science Rev.* 154, 72–101. doi: 10.1016/j.earscirev.2015.12.003

Gong, C., Sztanó, O., Steel, R. J., Xian, B., Galloway, W. E., and Bada, G. (2019b). Critical differences in sediment delivery and partitioning between marine and lacustrine basins: A comparison of marine and lacustrine aggradational to progradational clinothem pairs. *GSA Bull.* 131, 766–781. doi: 10.1130/B32042.1

Gong, C., Wang, Y., Steel, R. J., Olariu, C., Xu, Q., Liu, X., et al. (2015). Growth styles of shelf-margin clinoforms: prediction of sand-and sediment-budget partitioning into and across the shelf. *J. Sedimentary Res.* 85, 209–229. doi: 10.2110/jsr.2015.10

Hampson, G. J., and Storms, J. E. A. (2003). Geomorphological and sequence stratigraphic variability in wave-dominated, shoreface-shelf parasequences. *Sedimentology* 50, 667–701. doi: 10.1046/j.1365-3091.2003.00570.x

Harris, P. T., and Whiteway, T. (2011). Global distribution of large submarine canyons: Geomorphic differences between active and passive continental margins. *Mar. Geology* 285, 69–86. doi: 10.1016/j.margeo.2011.05.008

He, Y., Xie, X., Kneller, B. C., Wang, Z., and Li, X. (2013). Architecture and controlling factors of canyon fills on the shelf margin in the Qiongdongnan Basin, northern South China Sea. *Mar. Petroleum Geology* 41, 264–276. doi: 10.1016/j.marpetgeo.2012.03.002

Helland-Hansen, W., and Hampson, G. J. (2009). Trajectory analysis: concepts and applications. *Basin Res.* 21, 454–483. doi: 10.1111/j.1365-2117.2009.00425.x

Huang, K., Zhong, G., He, M., Zhu, W., and Wu, Z. (2024). Migration and controls of shenhu submarine canyons in the upper continental slope of northern south China sea: insights from three-dimensional seismic data mapping. *Sedimentology* 71, 2009–2034. doi: 10.1111/sed.13201

Jiang, T., Cao, L., Xie, X., Wang, Z., Li, X., Zhang, Y., et al. (2015). Insights from heavy minerals and zircon U–Pb ages into the middle Miocene–Pliocene provenance evolution of the Yinggehai Basin, northwestern South China Sea. *Sedimentary Geology* 327, 32–42. doi: 10.1016/j.sedgeo.2015.07.011

Johannessen, E. P., and Steel, R. J. (2005). Shelf-margin clinoforms and prediction of deepwater sands. *Basin Res.* 17, 521–550. doi: 10.1111/j.1365-2117.2005.00278.x

Jones, G. E. D., Hodgson, D. M., and Flint, S. S. (2015). Lateral variability in clinoform trajectory, process regime, and sediment dispersal patterns beyond the shelf-edge rollover in exhumed basin margin-scale clinothems. *Basin Res.* 27, 657–680. doi: 10.1111/bre.12092

Koo, W. M., Olariu, C., Steel, R. J., Olariu, M. I., Carvajal, C. R., and Kim, W. (2016). Coupling between shelf-edge architecture and submarine-fan growth style in A supply-dominated margin. *J. Sedimentary Res.* 86, 613–628. doi: 10.2110/jsr.2016.42

Li, C., Chen, G., Zhou, Q., Li, C., Sun, R., Lyu, C., et al. (2021). Multistage geomorphic evolution of the Central Canyon in the Qiongdongnan Basin, NW South China Sea. *Mar. Geophys Res.* 42, 27. doi: 10.1007/s11001-021-09448-8

Li, X., Ge, J., Zhao, X., Qi, K., Jones, B. G., and Fang, X. (2024). Geochemistry of quaternary sediments in the northwestern south China sea: sediment provenance and mid-pleistocene transition. *Mar. Geol.* 477, 107371. doi: 10.1016/j.margeo.2024.107371

Li, C., Lv, C., Chen, G., Zhang, G., Ma, M., Shen, H., et al. (2017). Source and sink characteristics of the continental slope-parallel Central Canyon in the Qiongdongnan Basin on the northern margin of the South China Sea. *J. Asian Earth Sci.* 134, 1–12. doi: 10.1016/j.jseaes.2016.10.014

Liang, C., Xie, X., He, Y., Chen, H., Yu, X., Zhang, W., et al. (2020). Multiple sediment sources and topographic changes controlled the depositional architecture of a palaeoslope-parallel canyon in the Qiongdongnan Basin, South China Sea. *Mar. Petroleum Geology* 113, 104161. doi: 10.1016/j.marpetgeo.2019.104161

Lin, C., He, M., Steel, R. J., Zhang, Z., Li, H., Zhang, B., et al. (2018). Changes in inner- to outer-shelf delta architecture, Oligocene to Quaternary Pearl River shelf-margin prism, northern South China Sea. *Mar. Geology* 404, 187–204. doi: 10.1016/j.margeo.2018.07.009

Liu, Z., Colin, C., Li, X., Zhao, Y., Tuo, S., Chen, Z., et al. (2010). Clay mineral distribution in surface sediments of the northeastern South China Sea and surrounding fluvial drainage basins: Source and transport. *Mar. Geology* 277, 48–60. doi: 10.1016/j.margeo.2010.08.010

Liu, H., Lin, C., Zhang, Z., Zhang, B., Tian, H., Zhang, M., et al. (2022). Shelf-margin architecture and deposition variability across the mid-Pleistocene climate transition, northeastern South China Sea. *Mar. Geology* 443, 106690. doi: 10.1016/j.margeo.2021.106690

Liu, M., Liu, H., Van Loon, A. J., (Tom), Xu, J., Hao, S., and Zhang, Y. (2023). Analysis of the geometric characteristics of clinothems and the relationship with shelf-edge trajectories of the Plio-Pleistocene continental slope in the Qiongdongnan Basin, South China Sea. *Sedimentology* 70, 5–30. doi: 10.1111/sed.13028

Liu, J., Saito, Y., Wang, H., Yang, Z., and Nakashima, R. (2007). Sedimentary evolution of the Holocene subaqueous clinoform off the Shandong Peninsula in the Yellow Sea. *Mar. Geology* 236, 165–187. doi: 10.1016/j.margeo.2006.10.031

Liu, J., Sun, Z., Wang, Z., Sun, Z., Wang, Z., Zhao, Z., et al. (2015). The evolution of the slope breaks in Qiongdongnan Basin and their controlling factors. *Mar. Geophys Res.* 36, 211–226. doi: 10.1007/s11001-014-9246-4

Lyu, C., Li, C., Chen, G., Zhang, G., Ma, M., Zhang, Y., et al. (2021). Zircon U–Pb age constraints on the provenance of upper oligocene to upper miocene sandstones in the western qiongdongnan basin, south China sea. *Mar. Pet. Geol.* 126, 104891. doi: 10.1016/j.marpetgeo.2020.104891

Meng, M., Liang, J., Lu, J., Zhang, W., Kuang, Z., Fang, Y., et al. (2021). Quaternary deep-water sedimentary characteristics and their relationship with the gas hydrate accumulations in the Qiongdongnan Basin, Northwest South China Sea. *Deep Sea Res. Part I: Oceanographic Res. Papers* 177, 103628. doi: 10.1016/j.dsr.2021.103628

Miller, K. G., Browning, J. V., Schmelz, W. J., Kopp, R. E., Mountain, G. S., and Wright, J. D. (2020). Cenozoic sea-level and cryospheric evolution from deep-sea geochemical and continental margin records. *Sci. Adv.* 6, eaaz1346. doi: 10.1126/sciadv.aaz1346

Morley, C. K. (2016). Major unconformities/termination of extension events and associated surfaces in the south China seas: review and implications for tectonic development. *J. Asian Earth Sci.* 120, 62–86. doi: 10.1016/j.jseaes.2016.01.013

Patruno, S., and Helland-Hansen, W. (2018). Clinoforms and clinoform systems: Review and dynamic classification scheme for shorelines, subaqueous deltas, shelf edges and continental margins. *Earth-Science Rev.* 185, 202–233. doi: 10.1016/j.earscirev.2018.05.016

Patruno, S., Scisciani, V., Helland-Hansen, W., D'Intino, N., Reid, W., and Pellegrini, C. (2020). Upslope-climbing shelf-edge clinoforms and the stepwise evolution of the northern European glaciation (lower Pleistocene Eridanos Delta system, U.K. North Sea): When sediment supply overwhelms accommodation. *Basin Res.* 32, 224–239. doi: 10.1111/bre.12379

Paumard, V., Bourget, J., Payenberg, T., Ainsworth, B., Lang, S., Posamentier, H. W., et al. (2018). Shelf-margin architecture and shoreline processes at the shelf-edge: controls on sediment partitioning and prediction of deep-water deposition style. *ASEG Ext. Abstr.* 2018, 1–6. doi: 10.1071/ASEG2018abM2_3B

Paumard, V., Bourget, J., Payenberg, T., George, A. D., Ainsworth, R. B., Lang, S., et al. (2020). Controls on deep-water sand delivery beyond the shelf edge: accommodation, sediment supply, and deltaic process regime. *J. Sedimentary Res.* 90, 104–130. doi: 10.2110/jsr.2020.2

Pellegrini, C., Asioli, A., Bohacs, K. M., Drexler, T. M., Feldman, H. R., Sweet, M. L., et al. (2018). The Late Pleistocene Po River lowstand wedge in the Adriatic Sea: Controls on architecture variability and sediment partitioning. *Mar. Petroleum Geology* 96, 16–50. doi: 10.1016/j.marpetgeo.2018.03.002

Pellegrini, C., Patruno, S., Helland-Hansen, W., Steel, R. J., and Trincardi, F. (2020). Clinoforms and clinothems: Fundamental elements of basin infill. *Basin Res.* 32, 187–205. doi: 10.1111/bre.12446

Pellegrini, C., Sammartino, I., Schieber, J., Tesi, T., Paladini De Mendoza, F., Rossi, V., et al. (2024). On depositional processes governing along-strike facies variations of fine-grained deposits: unlocking the little ice age subaqueous clinothems on the adriatic shelf. *Sedimentology* 71, 941–973. doi: 10.1111/sed.13162

Pellegrini, C., Tesi, T., Schieber, J., Bohacs, K. M., Rovere, M., Asioli, A., et al. (2021). Fate of terrigenous organic carbon in muddy clinothems on continental shelves revealed by stratal geometries: Insight from the Adriatic sedimentary archive. *Global Planetary Change* 203, 103539. doi: 10.1016/j.gloplacha.2021.103539

Petersen, T. G. (2021). New sequence stratigraphic framework on a 'passive' margin: implications for the post-break-up depositional environment and onset of glaciomarine conditions in NE Greenland. *J. Geological Soc.* 178, jgs2020–128. doi: 10.1144/jgs2020-128

Ramon-Duenas, C., Rudolph, K. W., Emmet, P. A., and Wellner, J. S. (2018). Quantitative analysis of siliciclastic clinoforms: An example from the North Slope, Alaska. *Mar. Petroleum Geology* 93, 127–134. doi: 10.1016/j.marpetgeo.2018.02.013

Sanchez, C. M., Fulthorpe, C. S., and Steel, R. J. (2012). Miocene shelf-edge deltas and their impact on deepwater slope progradation and morphology, Northwest Shelf of Australia. *Basin Res.* 24, 683–698. doi: 10.1111/j.1365-2117.2012.00545.x

Septama, E., Bentley, S. J., and Droxler, A. W. (2016). Conduits, timing and processes of sediment delivery across a high-relief continental margin: Continental shelf to basin in Late Quaternary, Gulf of Papua. *Mar. Petroleum Geology* 72, 447–462. doi: 10.1016/j.marpetgeo.2016.02.009

Shepherd, J. W., Lang, S. C., Paumard, V., George, A. D., and Peyrot, D. (2023). Controls on shelf-margin architecture and sediment partitioning on the Hammerhead shelf margin (Bight Basin, southern Australia): Implications for Gondwanan break-up dynamics between Australia and Antarctica. *Earth-Science Rev.* 244, 104538. doi: 10.1016/j.earscirev.2023.104538

Shepherd, J. W., Paumard, V., Lang, S., and George, A. D. (2024). Investigating relationships between shoreline process regime, shelf-margin architecture, and deep-water sand delivery: insights from the early post-rift hammerhead shelf margin (bight basin, southern Australia). *Gondwana Res.* 135, 208–233. doi: 10.1016/j.gr.2024.07.023

Sun, Q., Wu, S., Lü, F., and Yuan, S. (2010). Polygonal faults and their implications for hydrocarbon reservoirs in the southern Qiongdongnan Basin, South China Sea. *J. Asian Earth Sci.* 39, 470–479. doi: 10.1016/j.jseaes.2010.04.002

Surlyk, F., and Larsen, M. (2023). Coarse-grained, marine, sub-wave base, high-angle clinoform sets: A little-known outcrop facies illustrated by Jurassic examples from East Greenland. *Basin Res.* 35, 1509–1529. doi: 10.1111/bre.12763

Sztanó, O., Szafián, P., Magyar, I., Horányi, A., Bada, G., Hughes, D. W., et al. (2013). Aggradation and progradation controlled clinothems and deep-water sand delivery model in the neogene lake pannon, Makó trough, pannonian basin, SE Hungary. *Global Planet. Change* 103, 149–167. doi: 10.1016/j.gloplacha.2012.05.026

Trincardi, F., Amorosi, A., Bosman, A., Correggiari, A., Madricardo, F., and Pellegrini, C. (2020). Ephemeral rollover points and clinothem evolution in the modern Po Delta based on repeated bathymetric surveys. *Basin Res.* 32, 402–418. doi: 10.1111/bre.12426

Van Hoang, L., Clift, P. D., Schwab, A. M., Huuse, M., Nguyen, D. A., and Zhen, S. (2010). Large-scale erosional response of SE Asia to monsoon evolution reconstructed from sedimentary records of the Song Hong-Yinggehai and Qiongdongnan basins, South China Sea. *SP* 342, 219–244. doi: 10.1144/SP342.13

Wang, D., Wu, S., Qin, Z., Spence, G., and Lü, F. (2013). Seismic characteristics of the huaguang mass transport deposits in the qiongdongnan basin, south China sea: implications for regional tectonic activity. *Mar. Geol.* 346, 165–182. doi: 10.1016/j.margeo.2013.09.003

Wei, X., Yan, D., Luo, P., Jiang, P., Wang, H., Zhou, J., et al. (2020). Astronomically forced climate cooling across the Eocene–Oligocene transition in the Pearl River Mouth Basin, northern South China Sea. *Palaeogeography Palaeoclimatology Palaeoecol.* 558, 109945. doi: 10.1016/j.palaeo.2020.109945

Wolinsky, M. A., and Pratson, L. F. (2007). Overpressure and slope stability in prograding clinoforms: Implications for marine morphodynamics. *J. Geophys. Res.* 112, 2007JF000770. doi: 10.1029/2007JF000770

Xie, X., Müller, R. D., Li, S., Gong, Z., and Steinberger, B. (2006). Origin of anomalous subsidence along the Northern South China Sea margin and its relationship to dynamic topography. *Mar. Petroleum Geology* 23, 745–765. doi: 10.1016/j.marpetgeo.2006.03.004

Xie, X., Müller, R. D., Ren, J., Jiang, T., and Zhang, C. (2008). Stratigraphic architecture and evolution of the continental slope system in offshore Hainan, northern South China Sea. *Mar. Geology* 247, 129–144. doi: 10.1016/j.margeo.2007.08.005

Xu, S., Cong, F., Hao, F., Xu, C., Zou, H., Zhang, X., et al. (2018). Shelf-edge trajectory and sediment dispersal in a lacustrine setting: A case study from Qinnan Depression, Bohai Bay Basin, China. *Mar. Petroleum Geology* 91, 562–575. doi: 10.1016/j.marpetgeo.2018.01.027

Yuan, S., Lü, F., Wu, S., Yao, G., Ma, Y., and Fu, Y. (2009). Seismic stratigraphy of the qiongdongnan deep sea channel system, northwest south China sea. *Chin. J. Oceanol. Limnol.* 27, 250–259. doi: 10.1007/s00343-009-9177-0

Zhang, G., Feng, C., Yao, X., Ji, M., Yang, H., Qu, H., et al. (2021). Petroleum geology in deepwater settings in a passive continental margin of a marginal sea: a case study from the South China Sea. *Acta Geologica Sinica-English Edition* 95, 1–20. doi: 10.1111/1755-6724.14621

Zhang, M., Lin, C., He, M., Zhang, Z., Li, H., Feng, X., et al. (2019). Stratigraphic architecture, shelf-edge delta and constraints on the development of the Late Oligocene to Early Miocene continental margin prism, the Pearl River Mouth Basin, northern South China Sea. *Mar. Geology* 416, 105982. doi: 10.1016/j.margeo.2019.105982

Zhao, R., Chen, S., Olariu, C., Steel, R., Zhang, J., and Wang, H. (2019). A model for oblique accretion on the South China Sea margin; Red River (Song Hong) sediment transport into Qiongdongnan Basin since Upper Miocene. *Mar. Geology* 416, 106001. doi: 10.1016/j.margeo.2019.106001

Zhao, Z., Sun, Z., Liu, J., Pérez-Gussinyé, M., and Zhuo, H. (2018). The continental extension discrepancy and anomalous subsidence pattern in the western qiongdongnan basin, south China sea. *Earth Planet. Sci. Lett.* 501, 180–191. doi: 10.1016/j.epsl.2018.08.048

Zhao, Z., Sun, Z., Wang, Z., Sun, Z., Liu, J., and Zhang, C. (2015). The high resolution sedimentary filling in Qiongdongnan Basin, Northern South China Sea. *Mar. Geology* 361, 11–24. doi: 10.1016/j.margeo.2015.01.002

Zhao, Q., Zhu, H., Zhou, X., Liu, Q., Cai, H., and Gao, W. (2021). Continental margin sediment dispersal under geomorphic control in Xihu Depression, East China Sea Shelf Basin. *J. Petroleum Sci. Eng.* 205, 108738. doi: 10.1016/j.petrol.2021.108738

Zhuo, H., Wang, Y., Sun, Z., Wang, Y., Xu, Q., Hou, P., et al. (2019). Along-strike variability in shelf-margin morphology and accretion pattern: An example from the northern margin of the South China Sea. *Basin Res.* 31, 431–460. doi: 10.1111/bre.12329